AD-A041 081 ARMY ELECTRONICS COMMAND FORT MONMOUTH N J F/G 4/1
CALCULATION OF SELECTED ATMOSPHERIC COMPOSITION PARAMETERS FOR --ETC(U)
MAY 77 H N BALLARD, J M SERNA, F P HUDSON

UNCLASSIFIED ECOM-5818 NL

| OF |
AD
A041 081

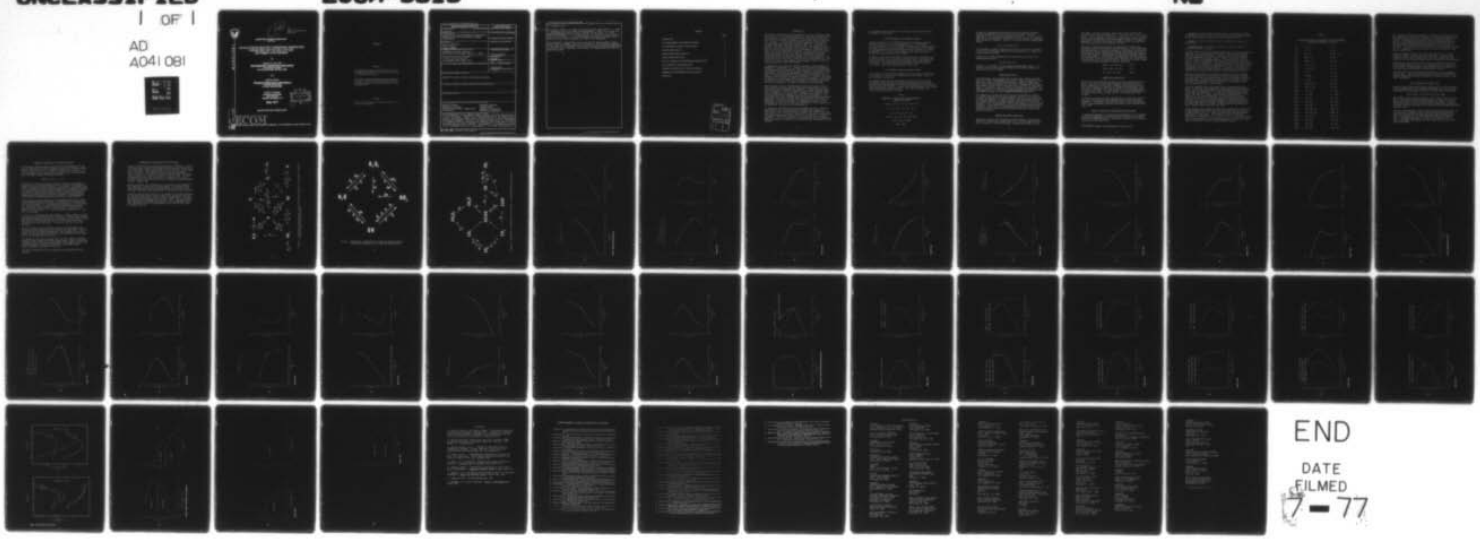

END

DATE
FILMED
7-77

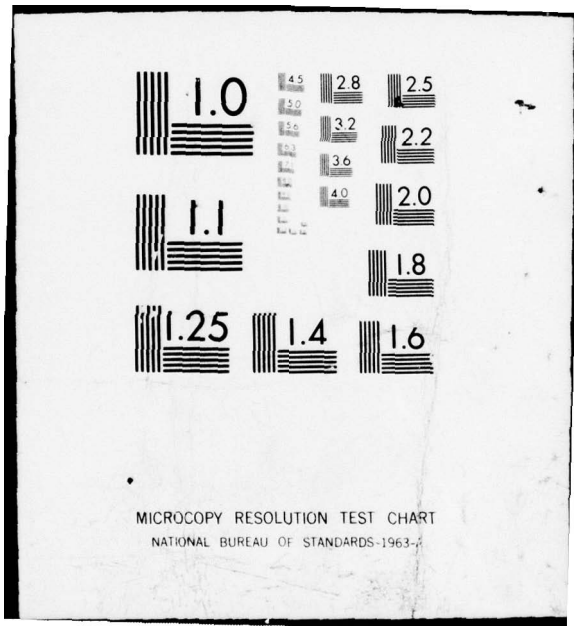
1.0
1.1
1.25
1.4
1.6
1.8
2.0
2.2
2.5
2.8
3.2
3.6
4.0
4.5
5.0
5.6
MICROCOPY RESOLUTION TEST CHART
NATIONAL BUREAU OF STANDARDS-1963-A

AD-A041 081

12

AD

Reports Control Symbol
OSD-1366

RESEARCH AND DEVELOPMENT TECHNICAL REPORT
ECOM-5818

CALCULATION OF SELECTED ATMOSPHERIC COMPOSITION PARAMETERS FOR THE MID-LATITUDE, SEPTEMBER STRATOSPHERE

By

HAROLD N. BALLARD
Atmospheric Sciences Laboratory
US Army Electronics Command
White Sands Missile Range, New Mexico 88002

and

JOSÉ M. SERNA
Physical Sciences Laboratory
New Mexico State University
Las Cruces, New Mexico 88001

FRANK P. HUDSON
Consultant for Chemical Kinetics
Sandia Laboratories
Albuquerque, New Mexico 87110

DDC
RECEIVED
JUN 30 1977
A

May 1977

Approved for public release; distribution unlimited.

DDC FILE COPY

ECOM
UNITED STATES ARMY ELECTRONICS COMMAND - FORT MONMOUTH, NEW JERSEY 07703

NOTICES

Disclaimers

The findings in this report are not to be construed as an official Department of the Army position, unless so designated by other authorized documents.

The citation of trade names and names of manufacturers in this report is not to be construed as official Government indorsement or approval of commercial products or services referenced herein.

Disposition

Destroy this report when it is no longer needed. Do not return it to the originator.

SECURITY CLASSIFICATION OF THIS PAGE *(When Data Entered)*

REPORT DOCUMENTATION PAGE

READ INSTRUCTIONS BEFORE COMPLETING FORM

1. REPORT NUMBER: ECOM-5818	2. GOVT ACCESSION NO.
3. RECIPIENT'S CATALOG NUMBER	
4. TITLE *(and Subtitle)*: CALCULATION OF SELECTED ATMOSPHERIC COMPOSITION PARAMETERS FOR THE MID-LATITUDE, SEPTEMBER STRATOSPHERE	5. TYPE OF REPORT & PERIOD COVERED
	6. PERFORMING ORG. REPORT NUMBER
7. AUTHOR(s): Harold N. Ballard, Jose M. Serna, Frank P. Hudson	8. CONTRACT OR GRANT NUMBER(s)
9. PERFORMING ORGANIZATION NAME AND ADDRESS: Atmospheric Sciences Laboratory, White Sands Missile Range, New Mexico 88002	10. PROGRAM ELEMENT, PROJECT, TASK AREA & WORK UNIT NUMBERS: 1L161102B53A-SA2
11. CONTROLLING OFFICE NAME AND ADDRESS: US Army Electronics Command, Fort Monmouth, New Jersey 07703	12. REPORT DATE: May 1977
	13. NUMBER OF PAGES: 48
14. MONITORING AGENCY NAME & ADDRESS *(if different from Controlling Office)*	15. SECURITY CLASS. *(of this report)*: UNCLASSIFIED
	15a. DECLASSIFICATION/DOWNGRADING SCHEDULE

16. DISTRIBUTION STATEMENT *(of this Report)*

Approved for public release; distribution unlimited.

17. DISTRIBUTION STATEMENT *(of the abstract entered in Block 20, if different from Report)*

18. SUPPLEMENTARY NOTES

19. KEY WORDS *(Continue on reverse side if necessary and identify by block number)*

Chemical kinetics
Atmospheric chemistry
STRATCOM (stratospheric composition)
Stratosphere
Atmospheric density
Computer model
Atmospheric composition
Modeling the atmosphere

20. ABSTRACT *(Continue on reverse side if necessary and identify by block number)*

The stratosphere is a very complex, highly variable, critically important part of man's environment. Progress in gaining understanding of its characteristics, behavior, and potential modification is based principally on field measurements of necessary parameters. Because of the complexity and variability, a mechanism for assembling field data and supporting laboratory data in the context of the applicable physical laws is required. This mechanism is by numerical simulation of the stratosphere by use of a large computer. This "model" approximation to

DD FORM 1 JAN 73 1473 EDITION OF 1 NOV 65 IS OBSOLETE

SECURITY CLASSIFICATION OF THIS PAGE *(When Data Entered)*

20. ABSTRACT (cont)

stratospheric behavior, in combining theory and actual measurements, is a powerful diagnostic tool in the study of the atmosphere. A model is very useful as an aid in developing both the general approach and the details of a field measurements program, and as an important tool in interpreting the experimental data of such a program. The interplay between measurements and model should produce the most effective approach to study of the stratosphere.

A few examples of calculational results from the ASL Numerical Model of Atmospheric Radiation (ANMAR), Composition and Dynamics, paralleling the conditions of the recent set of STRATCOM VI experiments, have been presented to demonstrate the range of results obtainable and the detail of treatment possible using the modeling approach.

CONTENTS

	Page
INTRODUCTION	2
FIELD MEASUREMENTS AND ATMOSPHERIC MODELS	3
THE ATMOSPHERIC CHEMICAL-KINETICS MODEL	3
COMPUTATIONAL RESULTS	4
COMPOSITION-PARTICLE DENSITIES	4
COMPOSITION-MIXING RATIOS	5
RATES OF CHEMICAL AND PHOTODISSOCIATION REACTIONS	5
TOTAL FORMATION AND REMOVAL RATES	8
TRANSPORT CONTRIBUTION TO PARTICLE DENSITIES	9
COMPARISON OF MEASUREMENTS AND CALCULATIONS	10
REFERENCES	41

INTRODUCTION

The chemical composition of the stratosphere is an ever-changing, highly variable result of the complex interplay of solar-induced photodissociation processes, resultant photochemical and thermochemical reactions, and a variety of transport processes on space scales ranging from molecular to global. The magnitude or relative importance of any process in determining composition and atmospheric behavior is dependent on altitude, latitude, time-of-day, season-of-year, and other variables. Because of the great complexity and variability, the fundamental requirement for gaining understanding of the stratosphere is measurement of a number of critical atmospheric parameters, including particle densities of key trace constituents, solar flux and thermodynamic properties. These measurements in themselves, however, do not provide explicit information of the processes which produced the results observed. They allow prediction of the state or behavior of the stratosphere only in a statistical sense if large numbers of measurements, under a variety of time and space conditions, are obtained.

A supplemental (and necessary) parallel approach is the development of mathematical simulations, i.e., "models," of stratospheric composition and behavior based on the physical laws which apply. Field measurements and theoretical speculation are the usual modes of motivation for model development, and laboratory measurements provide the quantization. A model is modified as required by the accumulation of relevant field measurements; and ultimately the degree-of-validity of a model is determined by comparison of calculated results with actual atmospheric measurements. The relative validity establishes the degree of confidence that can be placed on the diagnostic or predictive capabilities of the model.

During the past 8 years, the Atmospheric Sciences Laboratory (ASL) at White Sands Missile Range, NM, has developed a large, complex program of balloon-based stratospheric measurements in cooperation with several other laboratories. One of the central themes of this STRATCOM (STRATospheric COMposition) program [1] is simultaneous measurement of sets of related composition, thermodynamic and radiative parameters. Such measurement of related parameters under the same conditions allows direct, rather than statistical, analysis and interpretation of relationships. Development, testing and validation of computer-based models of the atmosphere can also be more direct, and confidence in their capabilities is enhanced by relating to actual measurements.

To support and supplement this field measurements program, a chemical-kinetic model of the stratosphere [2], incorporating a parametric application of the vertical transport processes, has recently been made operational at ASL. The model is used as one of the tools in developing the overall measurements program, as well as in designing individual experiments. It will also be used as an exploratory tool in theoretical studies to extend the capability of interpreting the experimental results obtained.

This document presents examples of the kinds of calculational results obtainable from the model.

FIELD MEASUREMENTS AND ATMOSPHERIC MODELS

A recent operation in the STRATCOM atmospheric measurements program, STRATCOM VI [3] was held in late September 1975. The principal set of measurements was in the altitude range of 25-39 kilometers during a 34-hour period on 24 and 25 September. A supporting set of IR absorption measurements was made from an altitude of 31 kilometers at sunset, 26 September 1975, using a second balloon. Both flights were from Holloman Air Force Base, NM, 32° N latitude.

To parallel these field measurements, the calculations, from which the following sample results are taken, were made by use of photolytic data derived from solar conditions for the latitude, dates, and altitudes given above. The photodissociation coefficients were calculated by J. L. Collins, and are presented and discussed in [4].

THE ATMOSPHERIC CHEMICAL-KINETICS MODEL

The structure and calculational method used in the computer simulation of stratospheric composition is discussed in greater detail in [2]. A brief summary is given here.

The computer model uses the Gear method of solution of sets of stiff differential equations [5] to solve the coupled continuity equations describing the time dependence of the particle densities of 30 chemically reactive atmospheric species. (Oxygen and nitrogen molecules are included with suitable steady-state densities.) The atoms, molecules, and radicals treated are given in Table 1.

TABLE 1

ATMOSPHERIC CHEMICAL SPECIES CONSIDERED IN COMPUTATIONAL MODEL

O $O(^1D)$ $O(^1S)$ O_2 $O_2(^1\Delta)$ $O_2(^1\Sigma)$ O_3

N N_2 NO NO_2 N_2O NO_3 N_2O_5

H H_2 OH H_2O HO_2 H_2O_2

CO CO_2 CH_2 CH_3 CH_4 CHO $HCHO$

CH_3O CH_3O_2 CH_3OOH

HNO_2 HNO_3

A total of 34 photodissociative processes and 115 chemical reactions, coupling the densities of the species, are considered. These are tabulated in [2] and partially sketched here in Figs. 1, 2, and 3, which show families of atmospheric constituents and the processes of conversion from one species to another. Figure 1 is for part of the nitrogen/oxygen family:

$$O,\ O_2,\ O_3,\ NO,\ NO_2,\ N_2O.$$

In the diagram, a chemical species at the tail of an arrow is converted to the one at the head by interaction with any species, or a photon ($h\nu$) listed on the arrow shaft.

Figure 2 is a similar representation of some of the reactions of the oxygen/hydrogen family:

$$OH,\ H_2O,\ HO_2,\ H_2O_2$$

Figure 3 is a limited set for the carbon/hydrogen/oxygen species. All reactions are not shown in these diagrams, and reactions linking the families are not all included.

COMPUTATIONAL RESULTS

The calculations, which produced the selected sample results presented below, were fully time-dependent and diurnal. Many calculations of this type use a number of equilibrium relationships and/or a steady-state solar input, and are therefore less realistic. Although the calculations were diurnal, and the results obtained are available for any time (day, night, or transition), only the results for noontime are presented. The following figures are therefore the model-derived characteristics of the stratosphere at noon, in late September at latitudes near 32° N.

The categories of calculated results chosen for presentation include: (1) particle densities of selected important species, (2) mixing ratios of these constituents, (3) rates of several sets of important photolytic and chemical reactions, (4) total formation and removal rates of some key species, and (5) equivalent transport contribution to a few molecular densities. All are presented as a function of altitude between 10 and 50 kilometers. Other types of information can be derived from the model, and equivalent results for other latitudes and periods of the year are readily calculable.

COMPOSITION-PARTICLE DENSITIES

Figures 4a to 4k are the calculated altitude profiles of the particle densities of ground-state oxygen atoms O (^3P), excited oxygen molecules $O_2(^1\Delta)$, ozone (O_3), nitric oxide (NO), nitrogen dioxide (NO_2), nitric

acid (HNO_3), nitrous oxide (N_2O), water (H_2O), carbon monoxide (CO), hydroxyl radical (OH) and methane (CH_4). (Units are cm^{-3}.) All of these species are of fundamental importance in stratospheric chemical kinetics, and all have been measured in the stratosphere. However, the number of measurements is very limited except for ozone and water, and even with these two, variability and uncertainty are high.

Figures 4ℓ to 4p are calculated particle densities of some of the speculative species which have not yet been detected in the stratosphere, but whose presence is required by photolytic and chemical considerations. These species include electronically excited oxygen atoms $O(^1D)$, perhydroxyl radicals (HO_2), hydrogen peroxide (H_2O_2), formaldehyde (HCHO) and nitrous acid (HNO_2). In the absence of measurements, the only information available on such constituents comes from models and related theory. In particular, the $O(^1D)$ atoms and the HO_2 radicals are involved in some critically important atmospheric reactions, including:

$$O(^1D) + H_2O \rightarrow OH + OH \qquad (73)^*$$

$$O(^1D) + N_2O \rightarrow NO + NO \qquad (71)$$

$$HO_2 + OH \rightarrow O_2 + H_2O \qquad (132)$$

COMPOSITION-MIXING RATIOS

Figures 5a to 5p present the same data as 4a to 4p expressed as mixing ratios: the particle density of the species divided by the total particle density of all the species present in the volume considered. This ratio of numbers of particles is termed the volume mixing ratio. The ratio of the masses (mass mixing ratio) is also frequently used, particularly for water. In these figures, the abscissa designation 10^{-6} is one part per million (1 ppmv), and 10^{-9} is one part per billion (1 ppbv).

The figures provide no new basic information, but allow direct consideration of the fraction of the atmosphere that a given constituent represents. They emphasize the fact that species which play dominant roles in many atmospheric processes are present in only extremely small proportions.

RATES OF CHEMICAL AND PHOTODISSOCIATION REACTIONS

To understand atmospheric characteristics and behavior, it is necessary to know what processes are occurring and the role and relative importance of each under the range of conditions encountered. As indicated previously, the processes are:

*The reaction numbers used throughout are as used in [2].

Radiative - concerned with the transmission, scattering, absorption and emission of energy in the infrared, visible, and ultraviolet regions, and the thermodynamic consequences on atomic/molecular scales.

Dynamic - covering the range of particle motions from molecular to global scales.

Chemical Kinetic - treating the multitude of chemical reactions among the many species present.

A useful method of deriving and demonstrating the role of various chemical reactions is to calculate the rate at which a given reaction proceeds under the conditions considered. Figures 6a to 6n are the calculated altitude dependencies of the rates of a number of important reactions for the noon, 32° N, September situation. The reactions are listed in Table 2. Some of the reactions are grouped to allow direct comparison of certain critical relationships. Since the relevance or role of a specific reaction or set of reactions is dependent on the particular problem under consideration, the following discussion will not be in the context of stratospheric pollution, weapons effects, meteorology, or other specific present concerns, but will be limited to a few brief general remarks.

Figure 6a shows the rates for the most important atmospheric reaction: the initial production of oxygen atoms by photodissociation of oxygen molecules, which sets the stage for most of the stratospheric chemistry of consequence. It should be noted how rapidly this photolysis falls off below 25 kilometers altitude - the rate at 10 kilometers is less than one thousandth that at 25 kilometers.

Figure 6b represents the two principal modes of photodissociation of ozone. In reaction 5 the products are ground-state atoms and molecules, while reaction 7 produces electronically excited (and more reactive) atoms $O(^1D)$ and molecules $O_2(^1\Delta)$. Reaction 5 dominates below 30 kilometers, and reaction 7 above. Ozone formation (reactions 36 + 37) is shown in Fig. 6c; and the comparison of this three-body formation rate with the photolytic destruction (the sum of reactions 5 and 7) is presented in Fig. 6d. It should be noted that these reaction rates are very large compared with other atmospheric reactions and that they are almost equal at all altitudes, so that an equilibrium among O, O_2 and O_3 closely follows the solar flux input.

Three important ways in which the oxygen atoms (produced in Fig. 6a and brought somewhat into equilibrium in Fig. 6d) enter into the chemistry is demonstrated in Fig. 6e. These are three of the principal removal mechanisms of oxygen atoms. The removal of O and O_3 by the much-publicized NO_x "catalytic" cycle is shown in Fig. 6f. The $O+NO_2$ reaction (43) is much slower over this altitude range and is therefore the rate-controlling reaction for this "ozone depletion" process.

TABLE 2

REACTIONS SELECTED TO ILLUSTRATE ALTITUDE-DEPENDENCE OF RATES FOR FIGURES OF SECTION 3

(1)	$O_2 + h\nu$	→	$O + O$
(5)	$O_3 + h\nu$	→	$O + O_2$
(7)	$O_3 + h\nu$	→	$O(^1D) + O_2(^1\Delta)$
(11)	$NO_2 + h\nu$	→	$O + NO$
(32)	$HNO_3 + h\nu$	→	$OH + NO_2$
(36)	$O + O_2 + O_2$	→	$O_3 + O_2$
(37)	$O + O_2 + N_2$	→	$O_3 + N_2$
(38)	$O + O_3$	→	$O_2 + O_2$
(43)	$O + NO_2$	→	$O_2 + NO$
(50)	$O + HO_2$	→	$O_2 + OH$
(71)	$O(^1D) + N_2O$	→	$NO + NO$
(73)	$O(^1D) + H_2O$	→	$OH + OH$
(94)	$O_3 + NO$	→	$O_2 + NO_2$
(95)	$O_3 + NO$	→	$O_2 + NO_2^*$
(101)	$O_3 + OH$	→	$O_2 + HO_2$
(115)	$NO + NO_3$	→	$NO_2 + NO_2$
(117)	$NO + HO_2$	→	$OH + NO_2$
(119)	$NO + HO_2 + M$	→	$HNO_3 + M$
(123)	$OH + NO_2 + M$	→	$HNO_3 + M$
(126)	$H + O_2 + M$	→	$HO_2 + M$
(132)	$OH + HO_2$	→	$O_2 + H_2O$
(134)	$OH + CO$	→	$H + CO_2$
(135)	$OH + CH_4$	→	$H_2O + CH_3$

Also important in the NO/O_3 problem, and the utlimate controlling factor when combined with HNO_3 dynamic removal, is the three-body formation and photolytic loss of nitric acid in reactions 123 and 32 as plotted in Fig. 6g. The balance among formation, loss, and transport removal of HNO_3 will help establish the NO_2 density since it will remove NO_2 from the equilibrium concentration that the reactions in Fig. 6h tend to establish. These are the rates for formation of NO_2 by the $NO+O_3$ reaction and for its photodissociative destruction. Below 35 kilometers, these are very nearly equal.

Figure 6i compares the $NO+O_3$ rate with other important nitric oxide reactions, showing its dominance at all altitudes. Figure 6j demonstrates the role of the excited oxygen atoms $O(^1D)$ produced by ozone photolysis as the principal primary source of OH radicals and NO molecules.

Figure 6k gives the rates for three of the most important reactions of these hydroxyl radicals, while Fig. 6ℓ shows their role in destruction of the natural and anthropogenic carbon monoxide (CO) and methane (CH_4) that move into the stratosphere from the earth's surface.

Figure 6m shows the principal formation mechanisms of the perhydroxyl radical (HO_2). Figure 6n compares formation of nitric acid from NO and from NO_2 showing the potential importance of the OH/NO_2 process in the lower stratosphere.

TOTAL FORMATION AND REMOVAL RATES

Figures 7a and 7b show the calculated noontime, 32° N latitude, September altitude dependencies of the formation and removal rates, by all applicable chemical and photolytic processes, for eight minor constituents:

$$O(^3P),\ O(^1D),\ O_3,\ NO,\ NO_2,\ OH,\ HO_2 \text{ and } HNO_3$$

The formation rate is essentially equal to the removal rate for all but HNO_3 in this near-equilibrium noontime situation. Hence, for all but HNO_3 only one curve is seen for both formation and removal. This was implied for ozone in Fig. 6d since the entire production of ozone is by reactions 36 and 37, and almost all of the loss is by the photodissociation reactions 5 and 7.

Figure 7a also demonstrates that oxygen atom formation-removal rates are virtually equal to those of ozone in the altitude range considered. Similarly the NO and NO_2 pair have essentially equal production-loss rates. The hydroxyl radical (OH) formation-removal rates shown in Fig. 7b are approximately equal to those of the perhydroxyl radical (HO_2) in the lower stratosphere, but are a small factor larger in the upper stratosphere.

TRANSPORT CONTRIBUTION TO PARTICLE DENSITIES

The continuity equations used to describe the time dependencies of the particle densities (n_i) of the atmospheric chemical constituents contain chemical formation terms (F_i), chemical and photolytic loss terms (L_i), and a divergence term to describe the net gain or loss of the particles due to transport through the volume considered:

$$\frac{d}{dt}[n_i] = F_i - L_i - \nabla\rho\bar{v}$$

The effect of the great variety of transport processes on atmospheric composition is very poorly understood, and is usually incorporated into models in somewhat artificial fashions. One purpose of the present model is to reverse this procedure, since the photolytic and chemical processes have been much better characterized, and derive mean characteristics of the vertical contribution to transport using atmospheric measurements combined with detailed chemical kinetic treatment. A preliminary part of this study is presented partially and briefly in Figs. 8a to 8e.

These figures show the regions of the stratosphere where the net result of the transport through the volume is an increase of the particle density (points plotted +) or a decrease (points plotted -). Alternatively, this can be described as a region where the chemical/photolytic loss rate is greater than the chemical formation rate (+), or where the formation rate is greater (-). The constituents considered are O_3, NO_2, N_2O, H_2O, and HNO_3.

In Fig. 8a, in the region above 30 kilometers altitude, removal of ozone by photolysis and reaction with NO, O, OH, etc., is faster than the three-body chemical formation, and ozone is transported into the region. Below the transition at 30 kilometers, there is a net formation and ozone transport is out from the region. The units of net loss or gain are $cm^{-3}\ sec^{-1}$.

For NO_2 (Fig. 8b), excess formation is above 17-19 kilometers, with deficient formation below and a net flow into the lower region. Nitrous oxide (N_2O) has a net chemical/photolytic loss throughout the stratosphere, and the equivalent contribution to the N_2O density by the upward flow is at the rates shown in Fig. 8c.

The reverse of this occurs for water (Fig. 8d) with chemical formation exceeding losses through the 10-50 kilometer range. Under the conditions considered, nitric acid losses dominate above 20 kilometers, with a flow upward and downward from the 10-20 kilometer region where there is excess formation, as indicated in Fig. 8e.

The results presented in Figs. 8a through 8e are exploratory and preliminary.

COMPARISON OF MEASUREMENTS AND CALCULATIONS

Results of some of the experimental measurements on STRATCOM VI reported in [3] have been plotted on the graphs of calculated particle densities and mixing ratios. These include ozone (Figs. 4c and 5c), nitrous oxide (Figs. 4g and 5g), carbon monoxide (Figs. 4j and 5j) and methane (Figs. 4k and 5k). It should be noted that since the model uses mean values as inputs, the results are plotted as smooth curves. The actual stratosphere can have sharp variations of a parameter over a small altitude interval, and an equivalent plot of measured altitude dependence could be a jagged line.

However, even with this consideration, the relatively good agreement of the computational results with the measurements for the given season, time, latitude, and altitude, gives some degree of confidence in the validity of the model and, consequently, in the other results calculated.

Similarly, some earlier results of J. G. Anderson, at the same latitude, for the short-lived highly reactive oxygen atoms and hydroxyl radicals are plotted comparatively in Figs. 4a and 4i, respectively. The oxygen atom results are for November 1974, 10:30 a.m. [6]. The length of the line indicates the experimental uncertainty. For the hydroxyl radical (OH), the dotted line is for measurements in July and the solid lines for January 1976 [7].

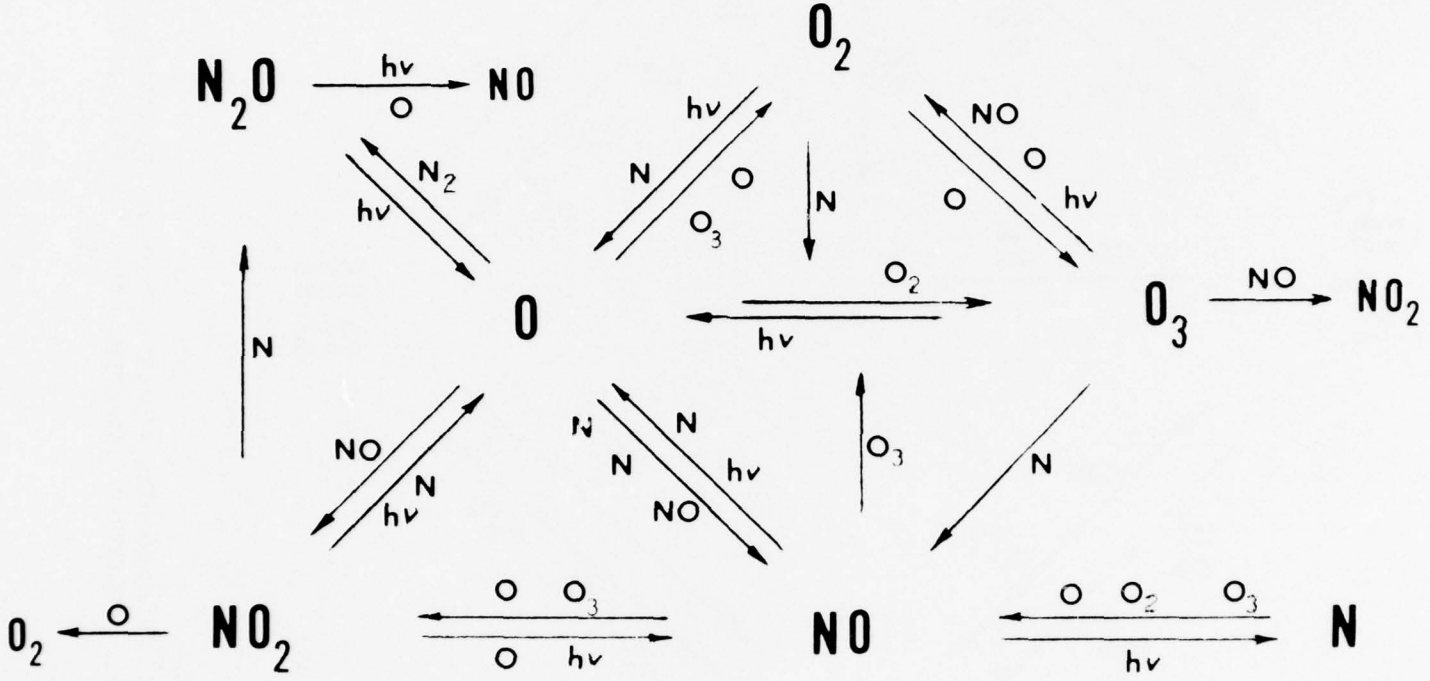

Figure 1. Diagrammatic representation of reactions among atmospheric constituents composed only of oxygen and nitrogen atoms.

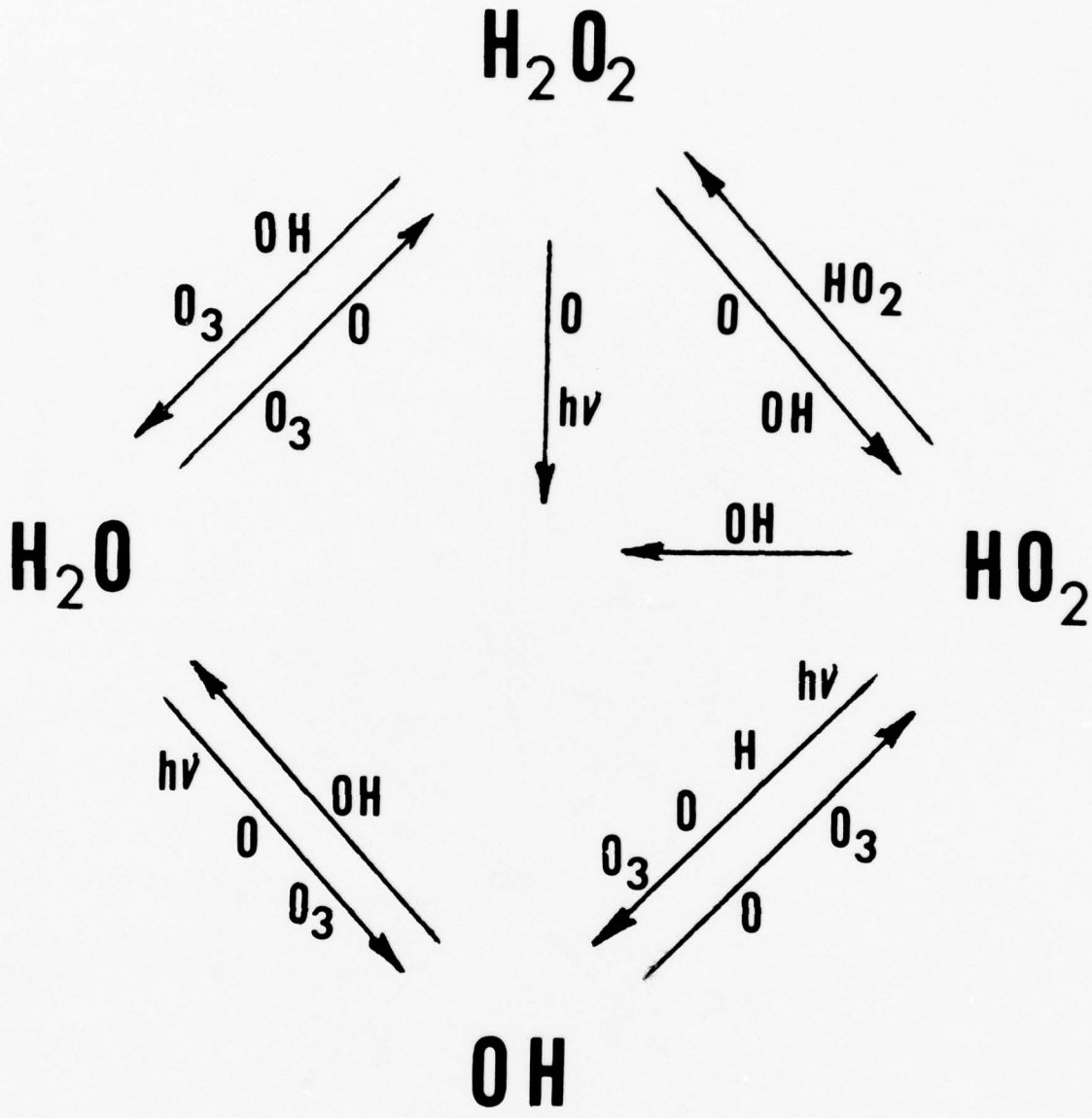

Figure 2. Diagrammatic representation of reactions among atmospheric constituents composed only of oxygen and hydrogen atoms.

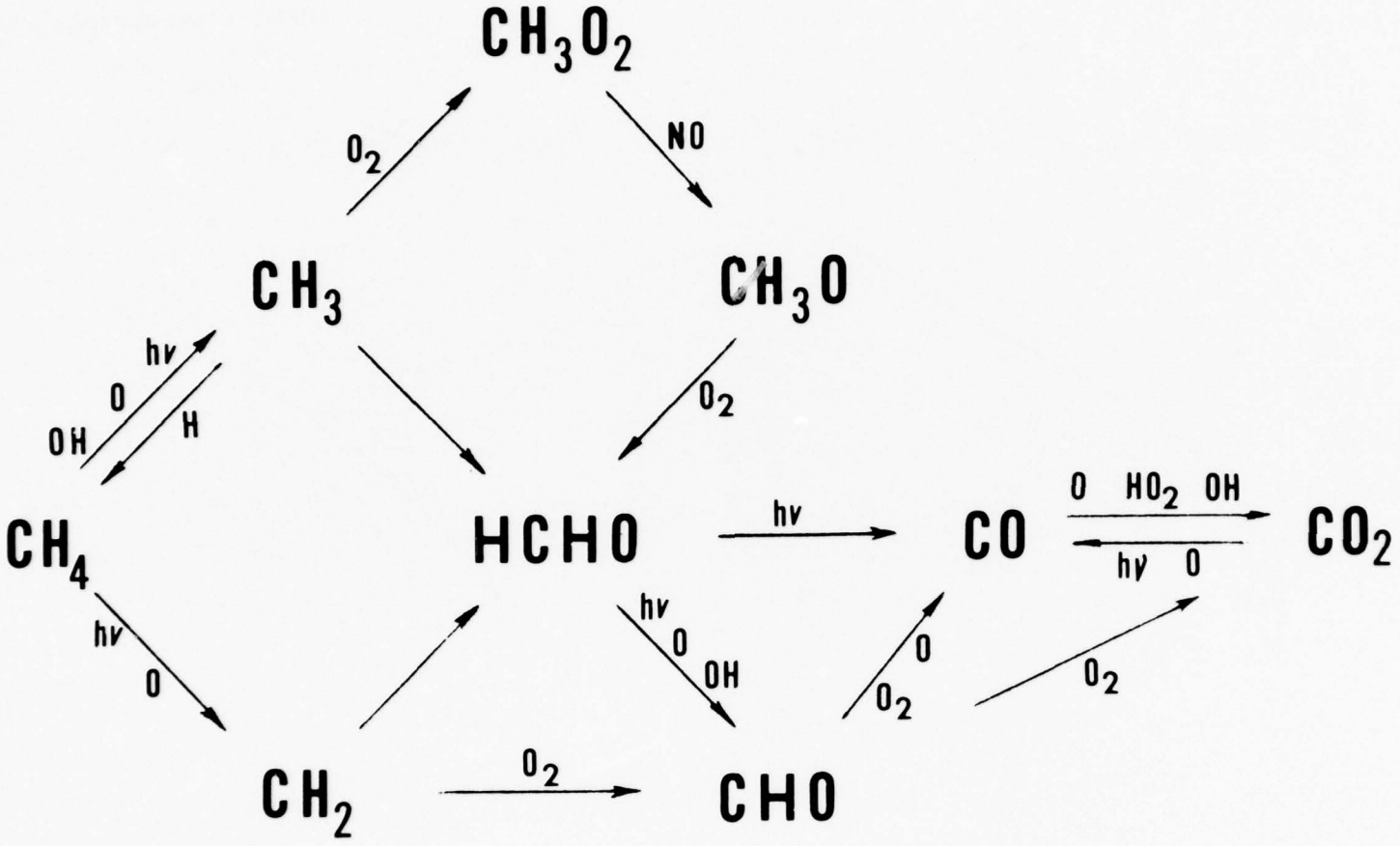

Figure 3. Diagrammatic representations of reactions of carbon/hydrogen/oxygen species.

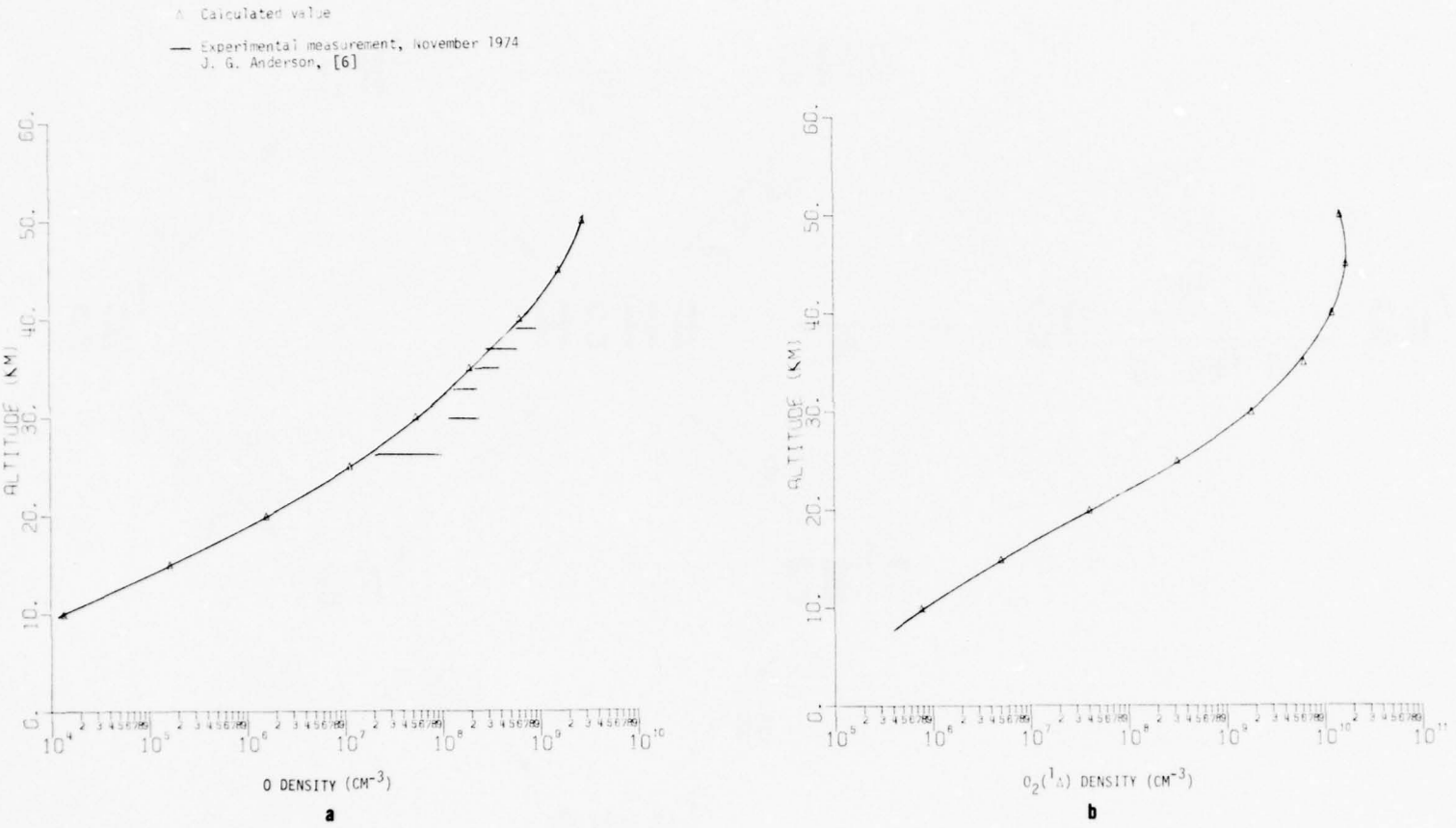

Figure 4. Composition-particle densities.

△ Calculated value

. Experimental measurement, STRATCOM VI

— Experimental measurement, Lowenstein, Sep 75 [8]

X Experimental measurement, Randhawa and Izquierdo, Sep 72 [9]

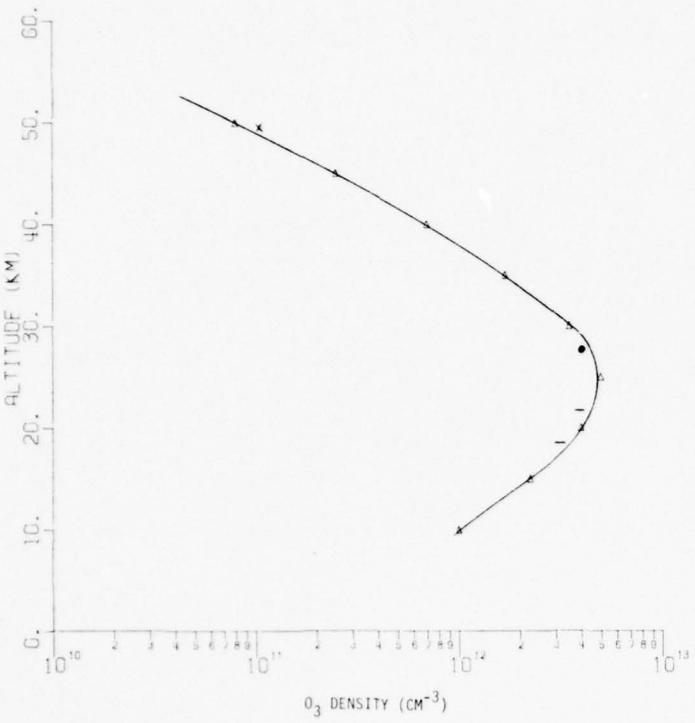

c

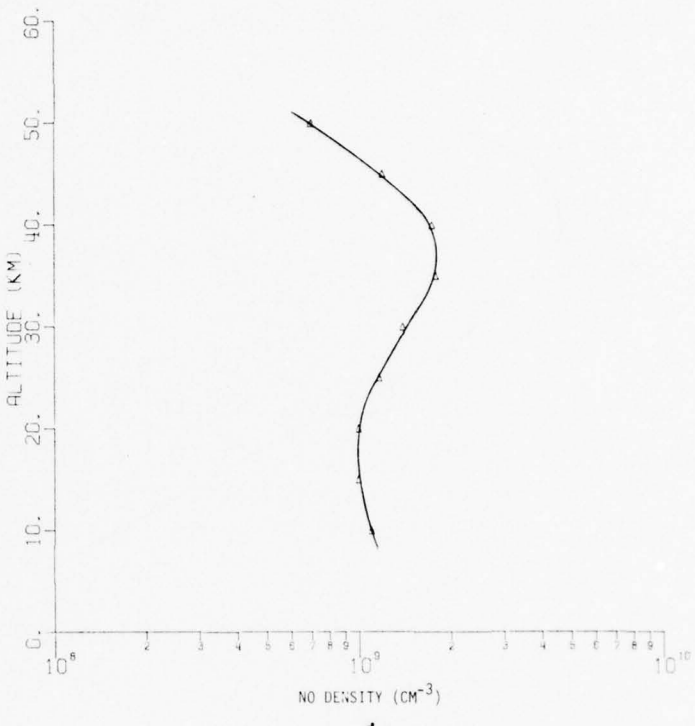

d

Figure 4. (cont)

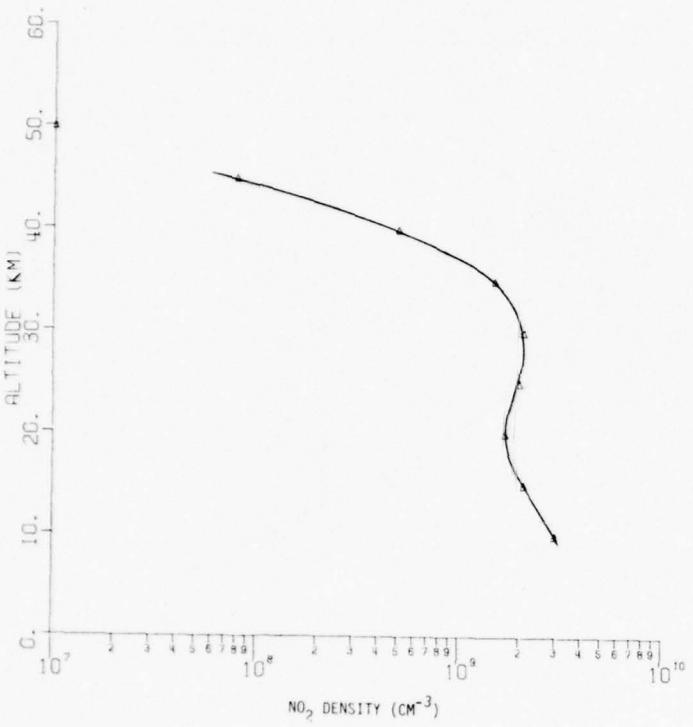

e

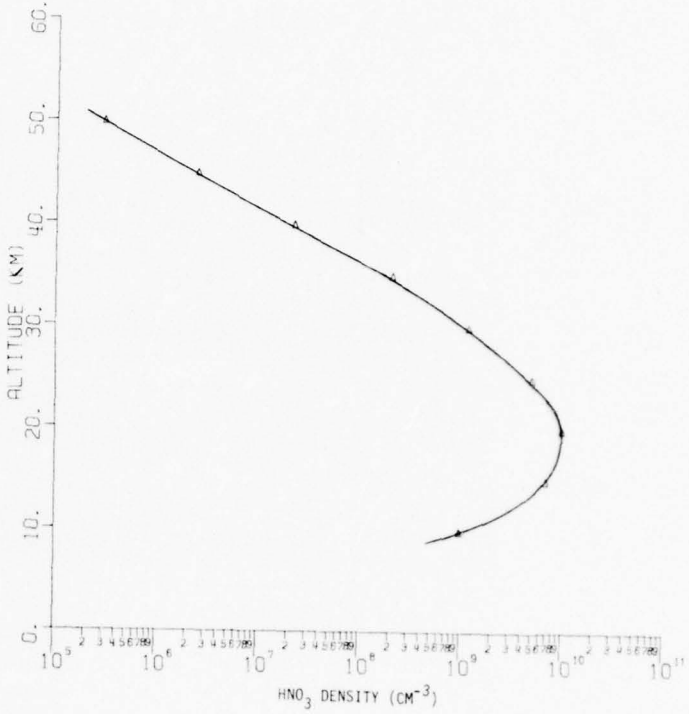

f

Figure 4. (cont)

△ Calculated value

. Experimental measurement, STRATCOM VI

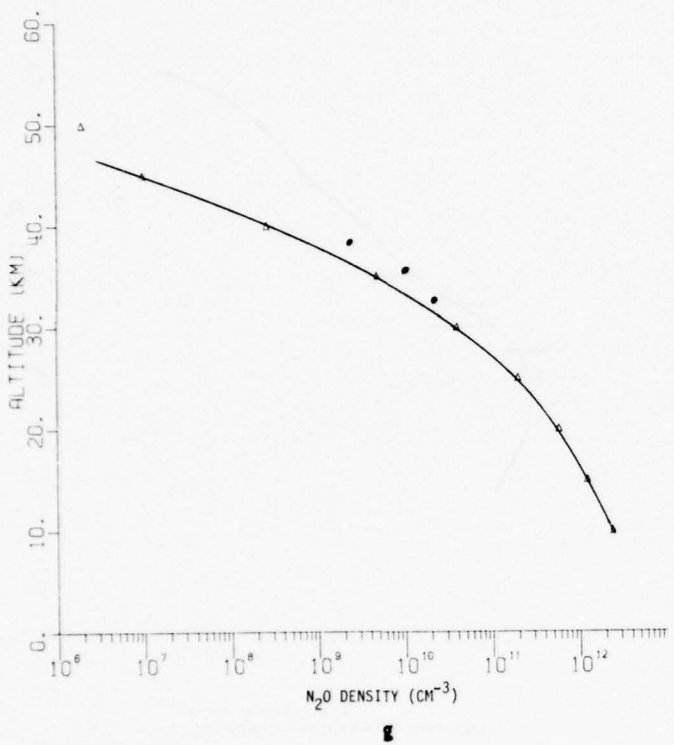

g

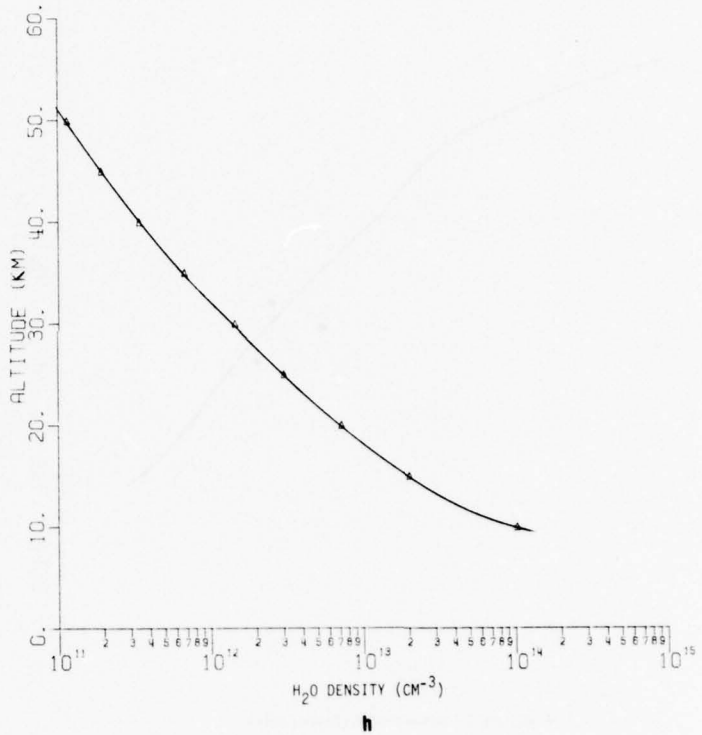

h

Figure 4. (cont)

Δ Calculated value

— Experimental measurement, January 1976
J. G. Anderson [7]

--- Experimental measurement, July 1975
J. G. Anderson [7]

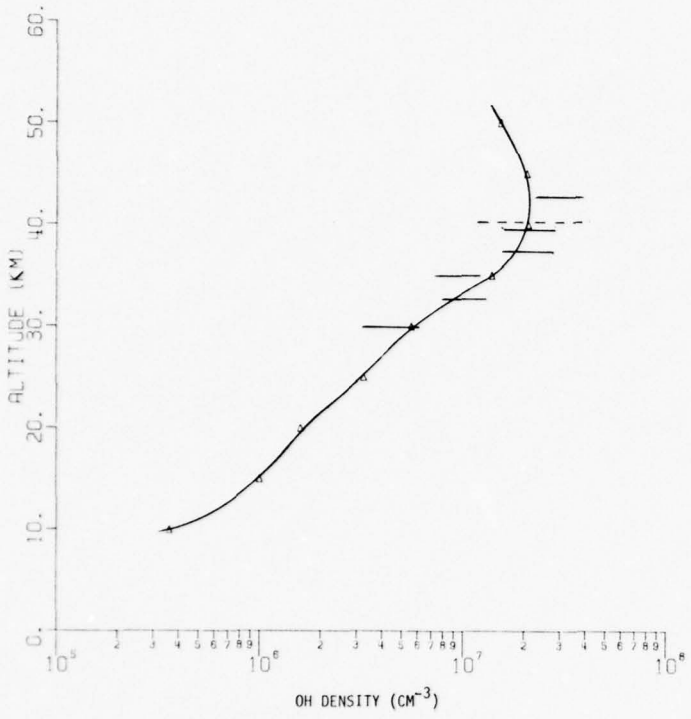

i

Δ Calculated value

. Experimental measurement, STRATCOM VI

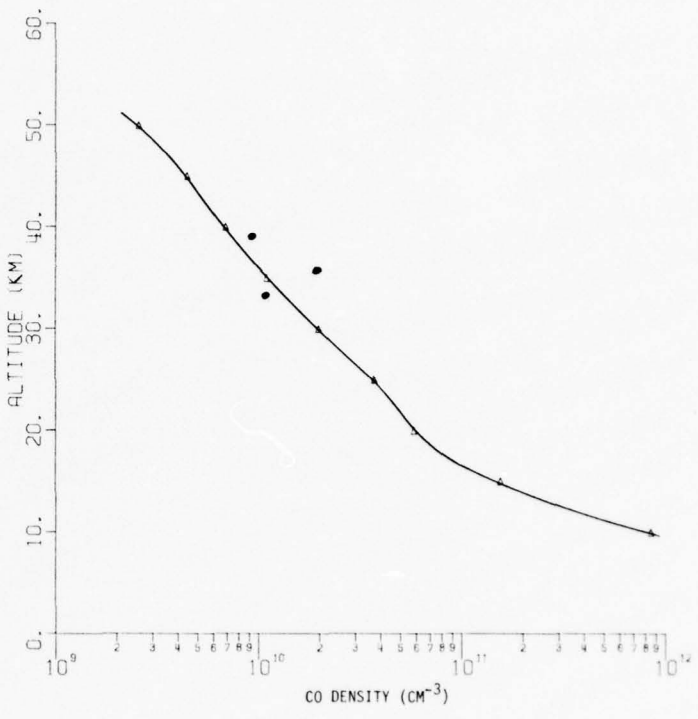

j

Figure 4. (cont)

Δ Calculated value

. Experimental measurement, STRATCOM VI

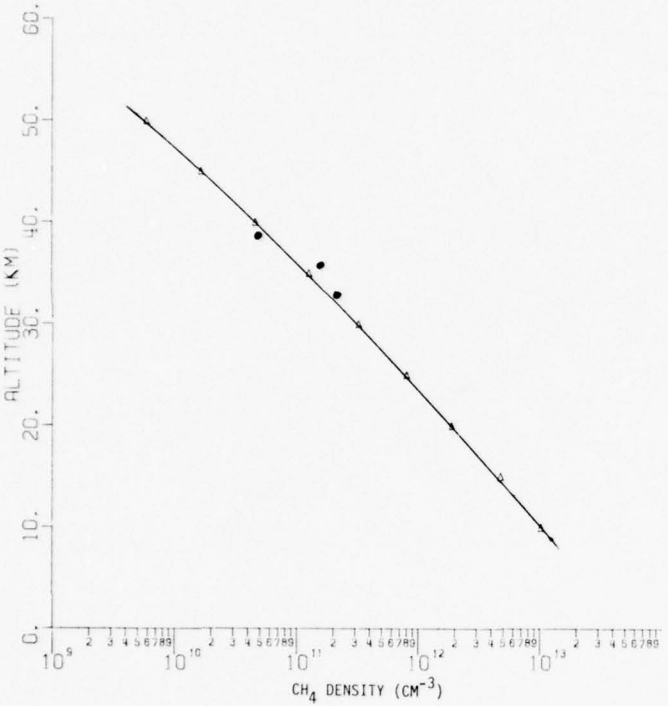

k

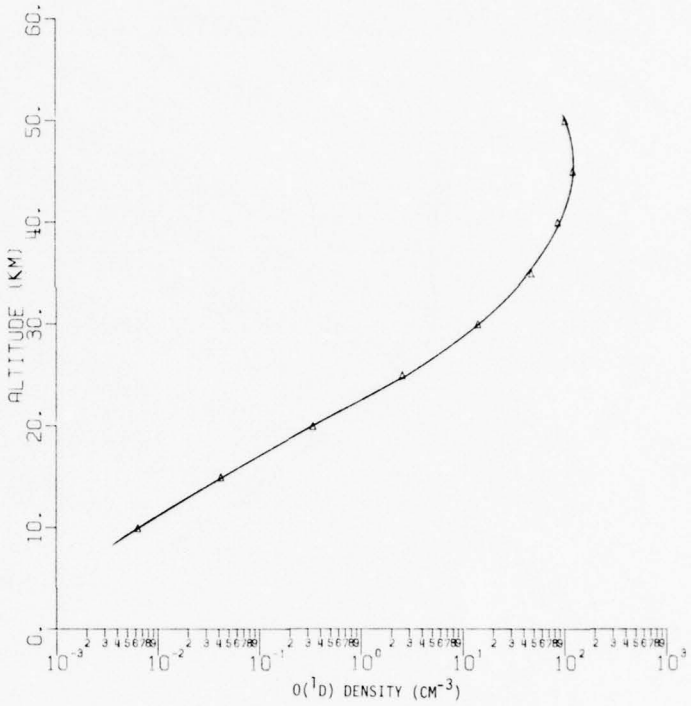

ℓ

Figure 4. (cont)

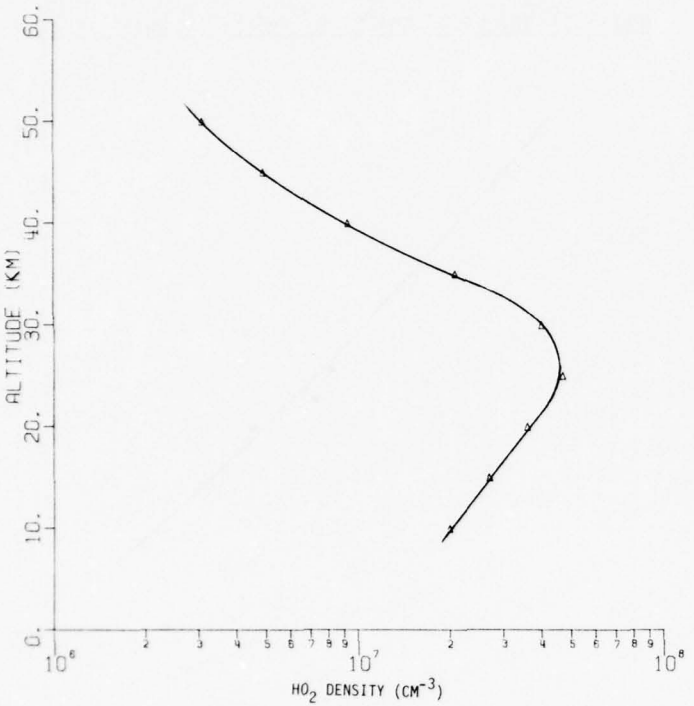

m

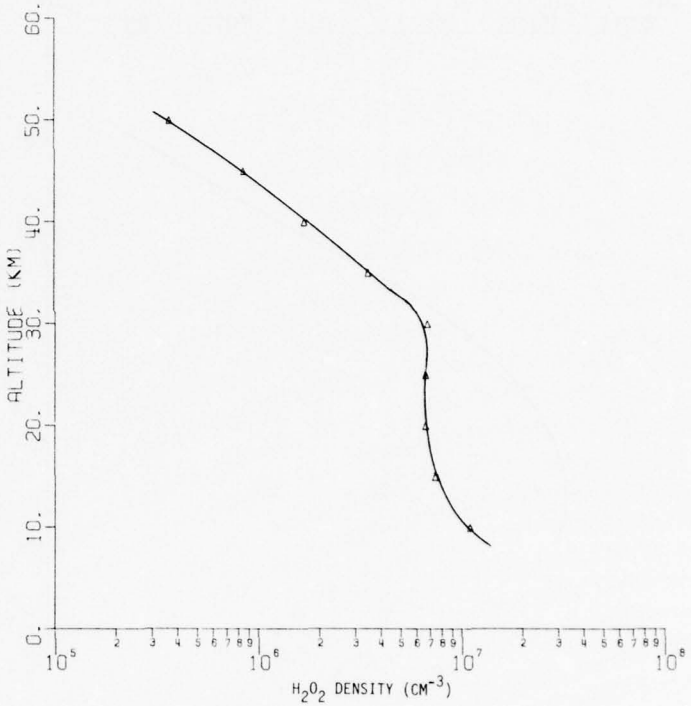

n

Figure 4. (cont)

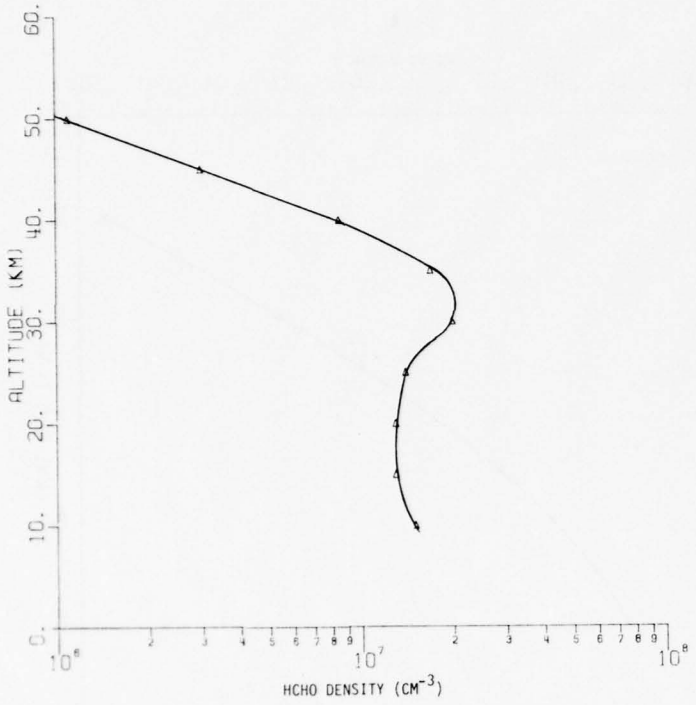

o

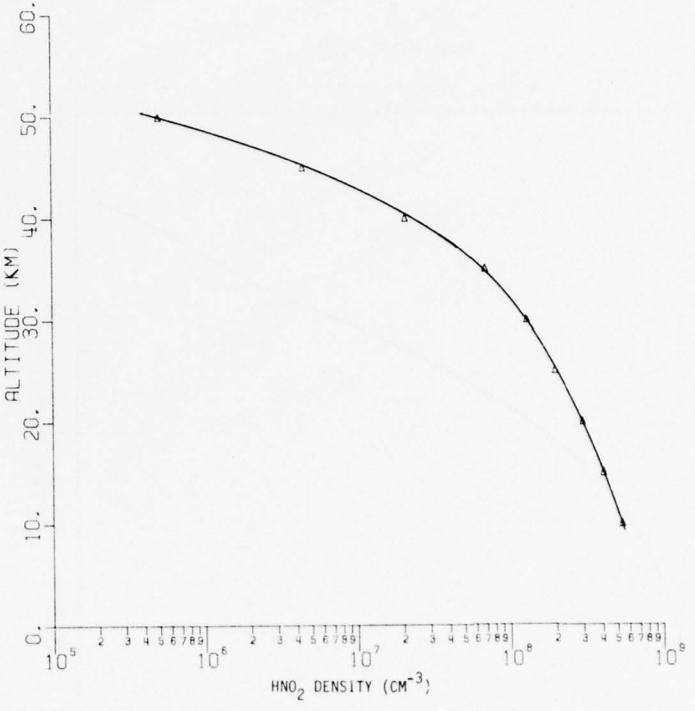

p

Figure 4. (cont)

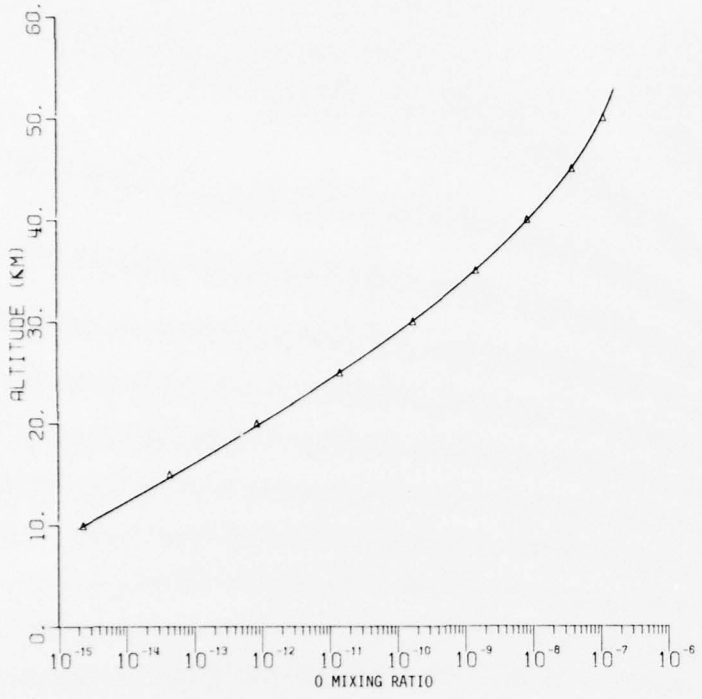

a

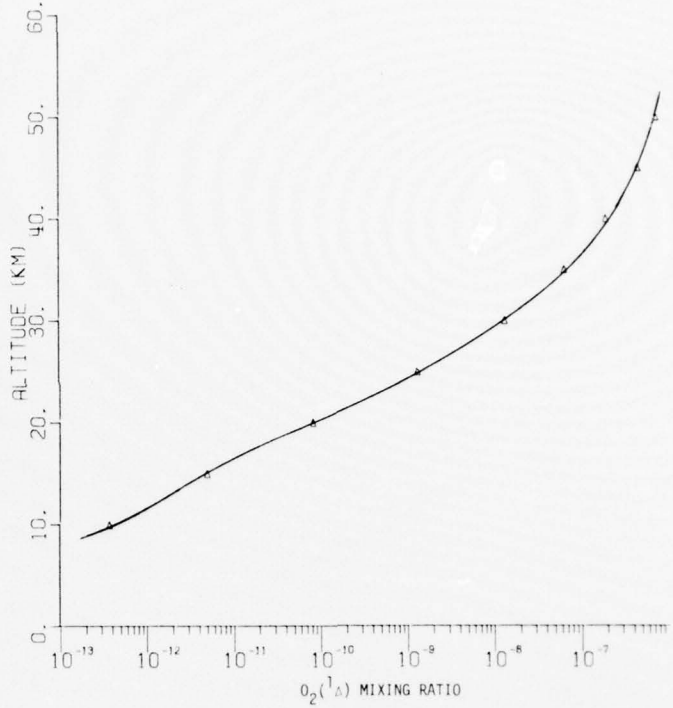

b

Figure 5. Composition-mixing ratios.

△ Calculated value

— Experimental measurement, Lowenstein, Sep 75 [8]

X Experimental measurement, Randhawa and Izquierdo, Sep 72 [9]

. Experimental measurement, STRATCOM VI

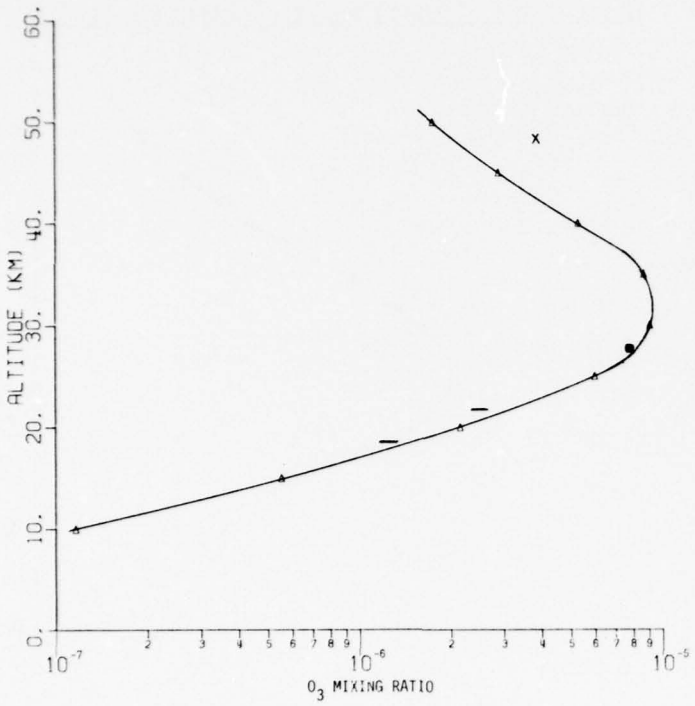

c

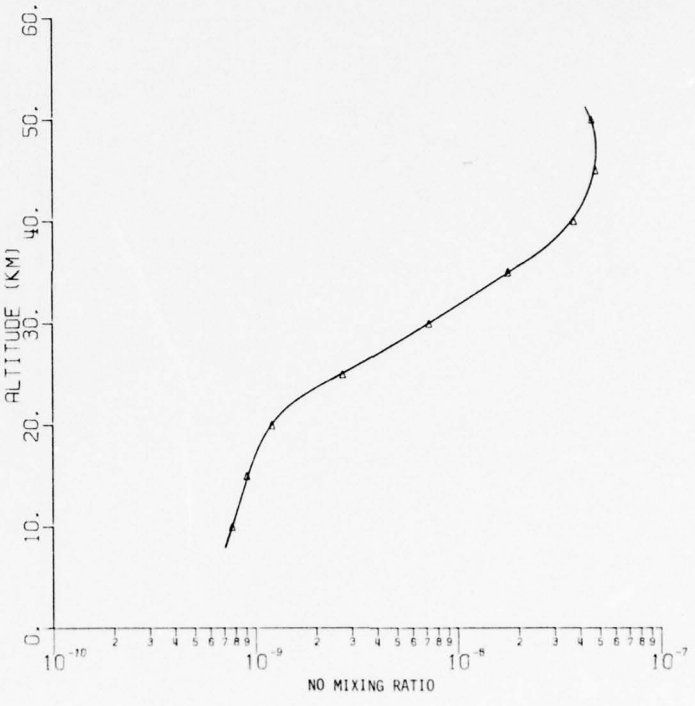

d

Figure 5. (cont)

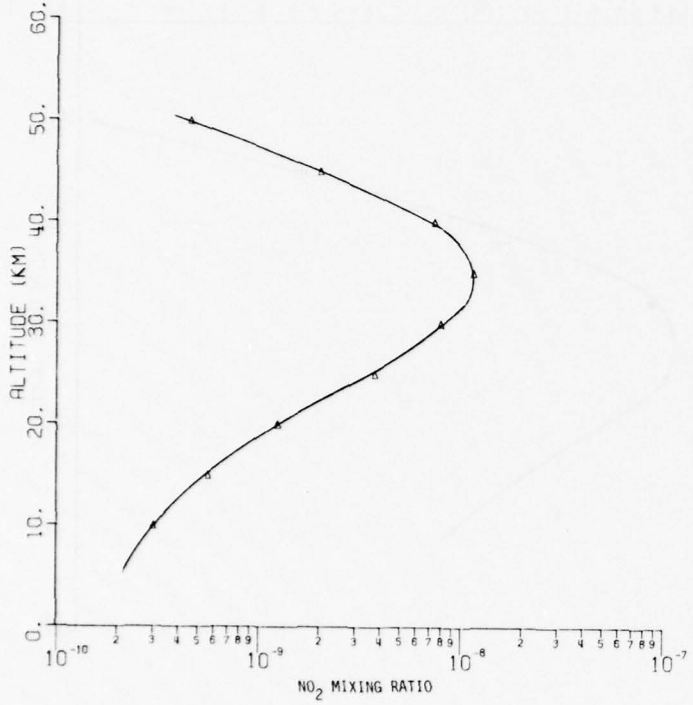

e

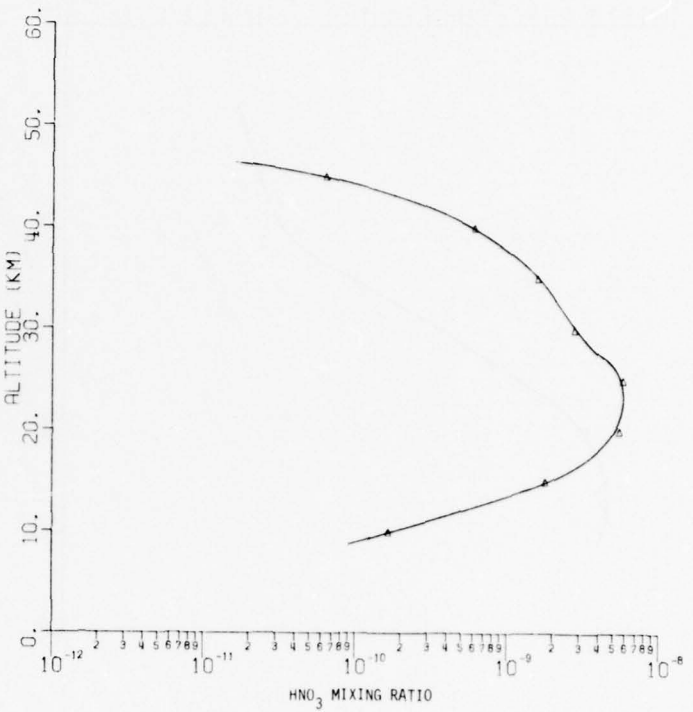

f

Figure 5. (cont)

Δ Calculated value

. Experimental measurement, STRATCOM VI

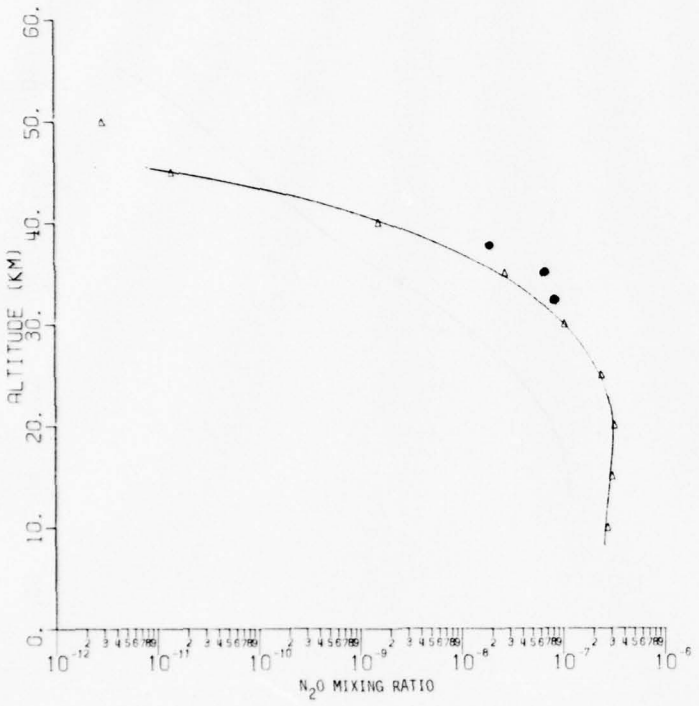

g

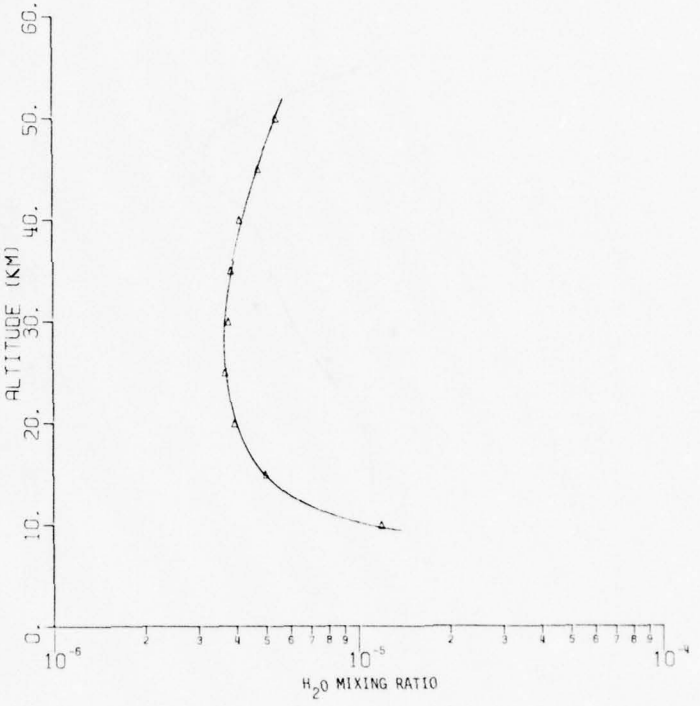

h

Figure 5. (cont)

Δ Calculated value

. Experimental measurement, STRATCOM VI

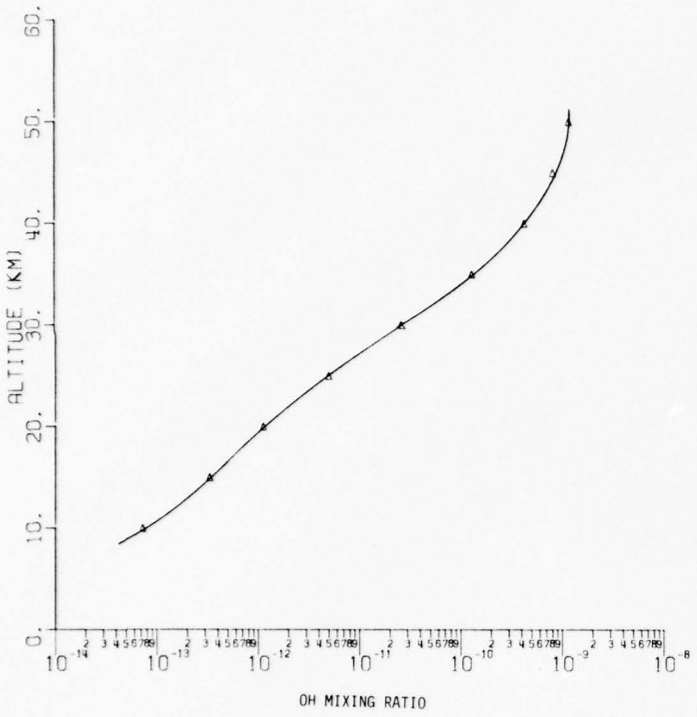

i

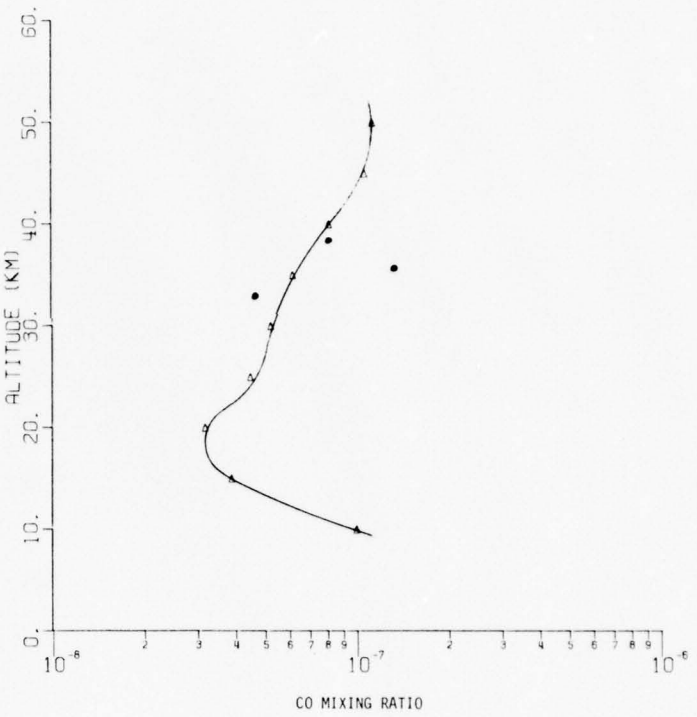

j

Figure 5. (cont)

△ Calculated value

. Experimental measurement, STRATCOM VI

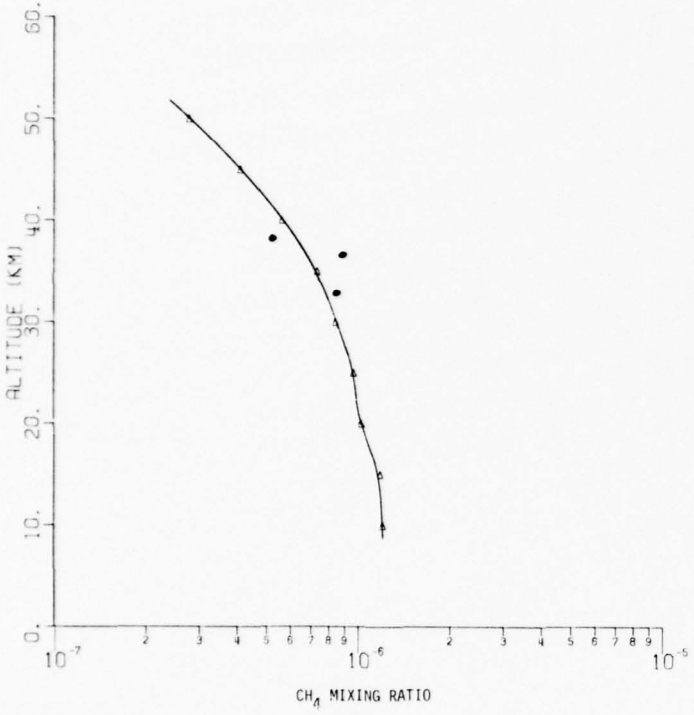

k

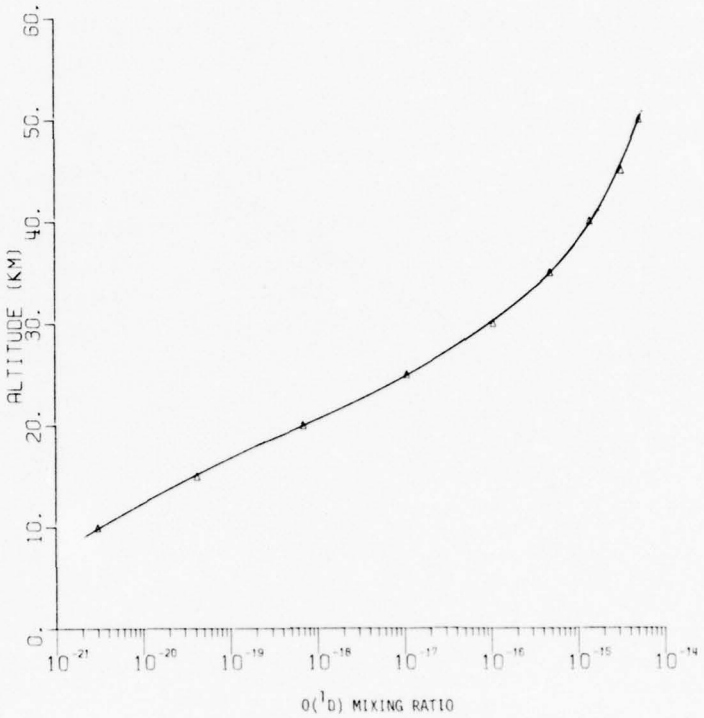

ℓ

Figure 5. (cont)

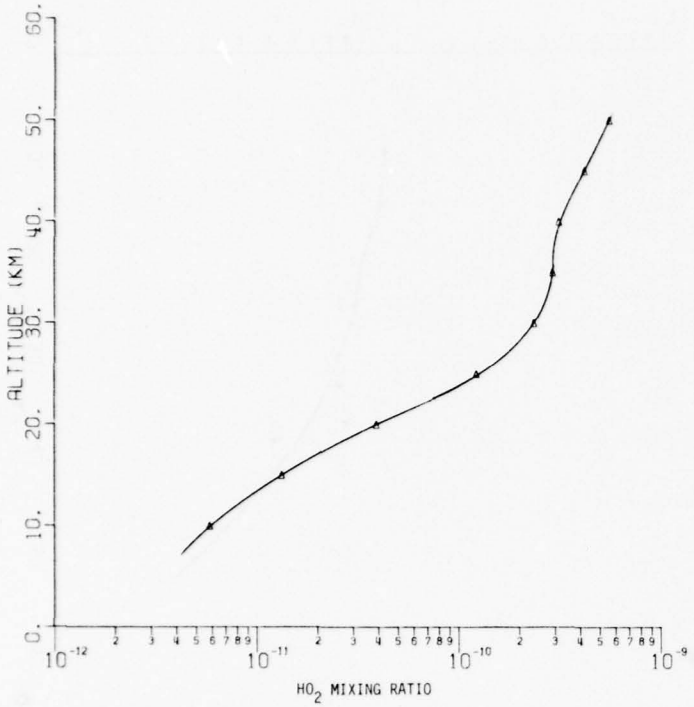

m

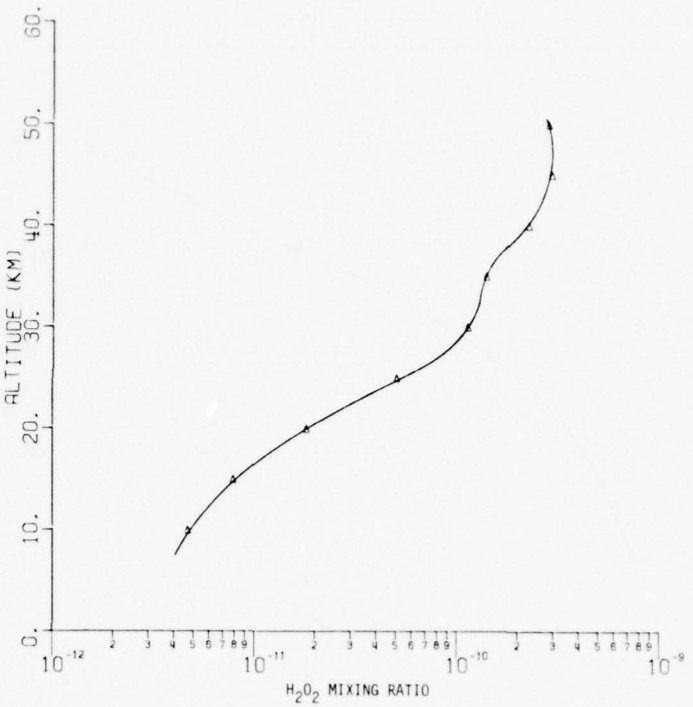

n

Figure 5. (cont)

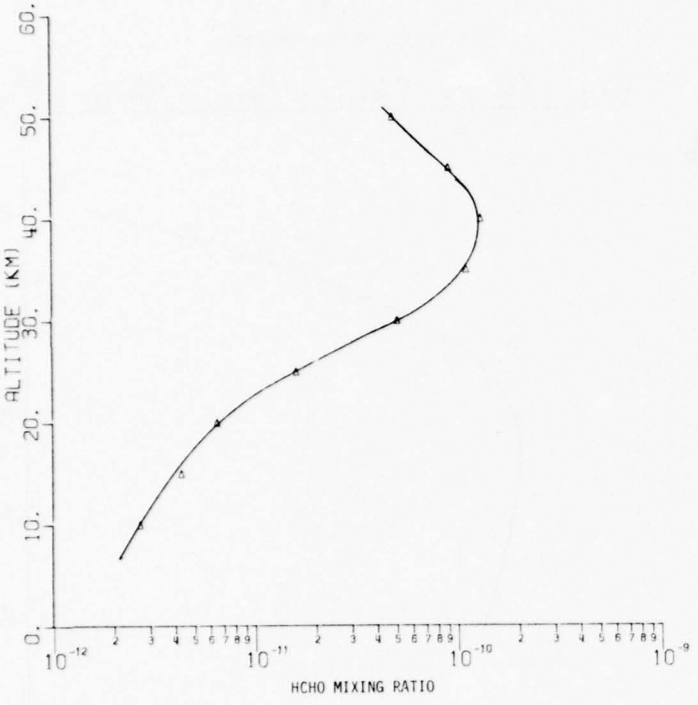

o

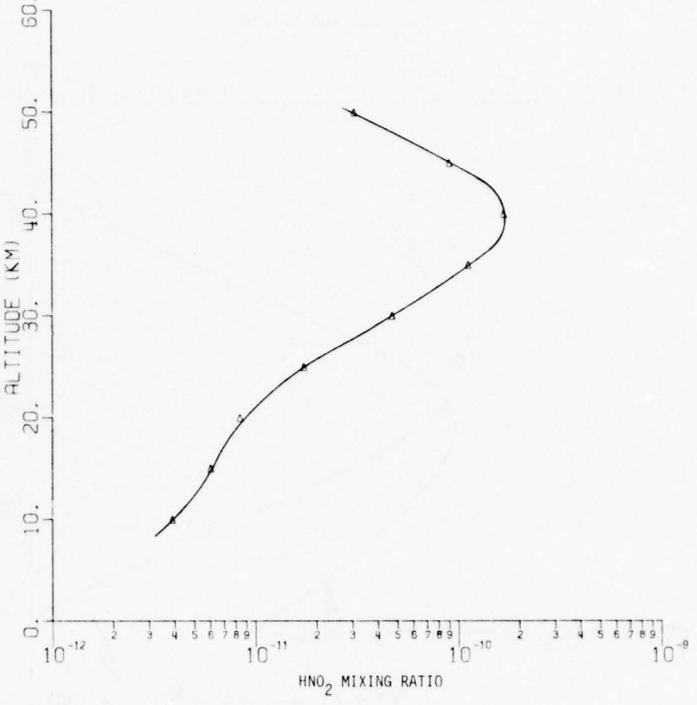

p

Figure 5. (cont)

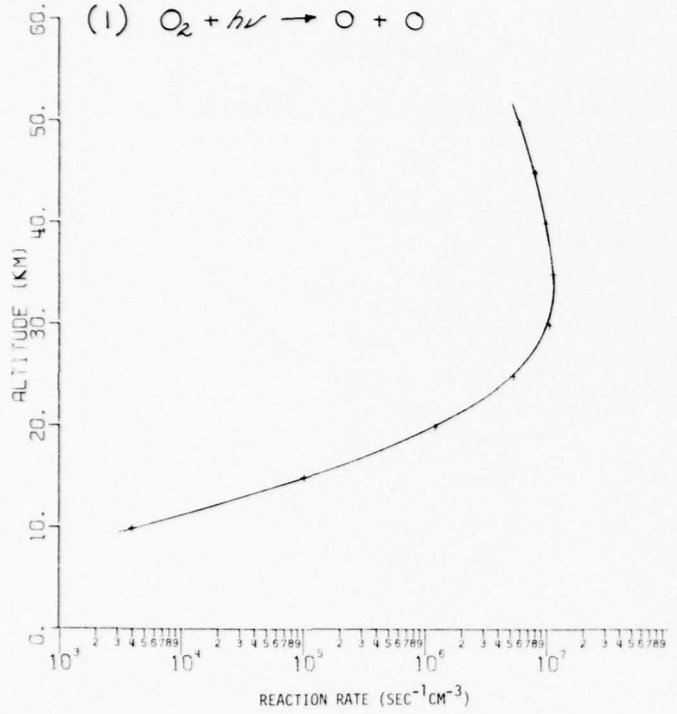

a

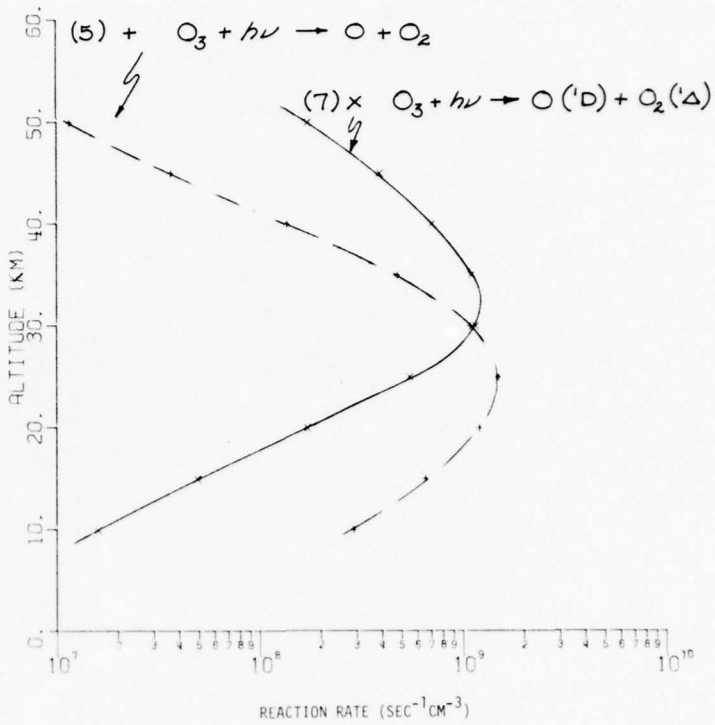

b

Figure 6. Rates of chemical and photodissociation reactions.

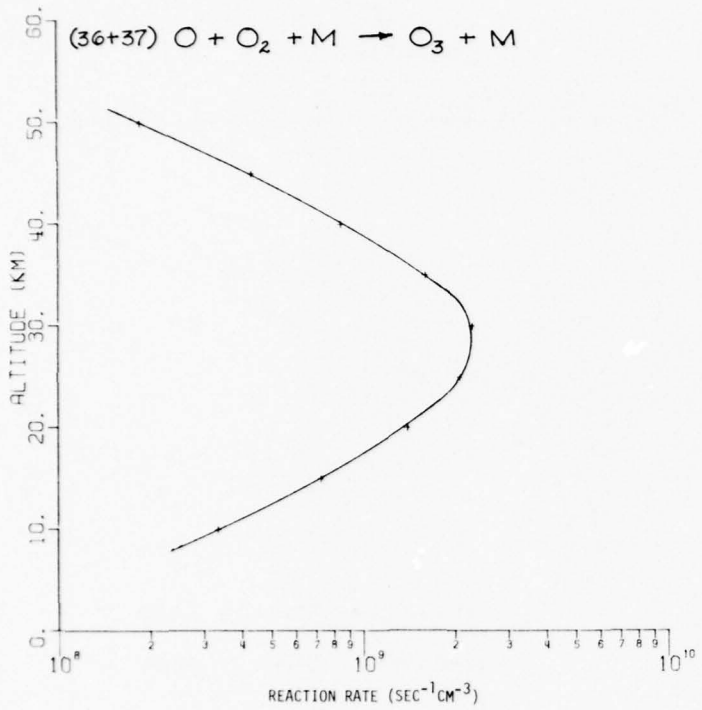

c

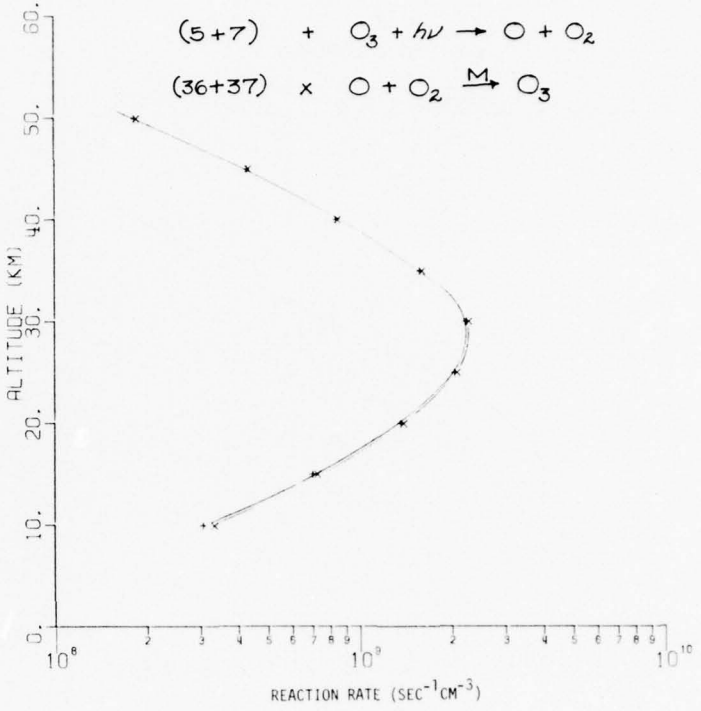

d

Figure 6. (cont)

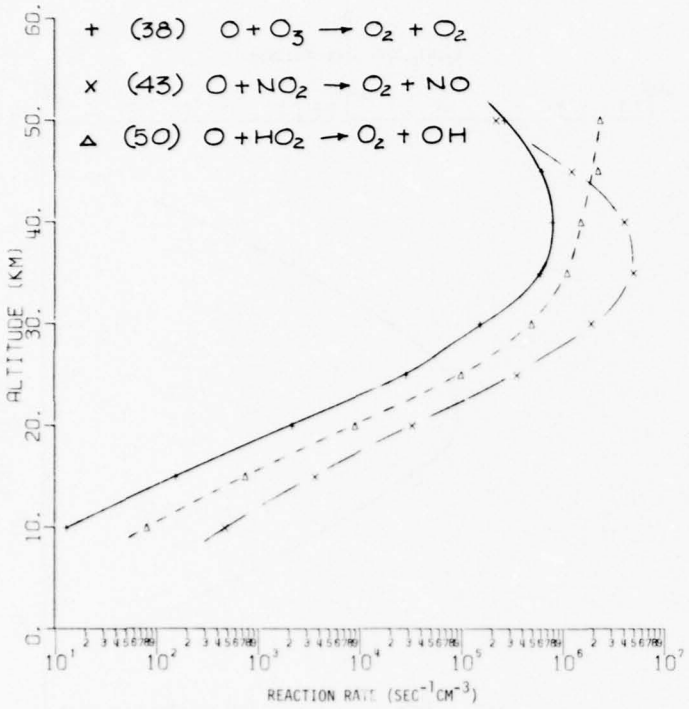

e

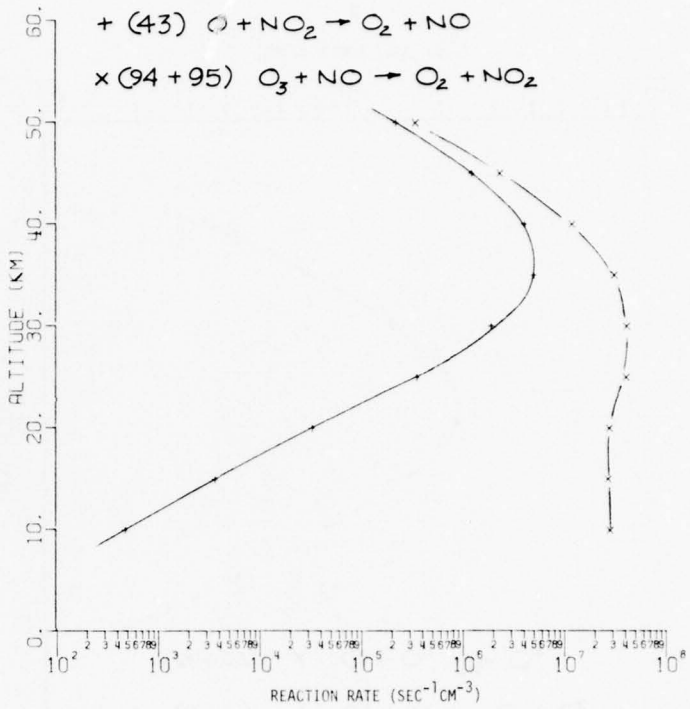

f

Figure 6. (cont)

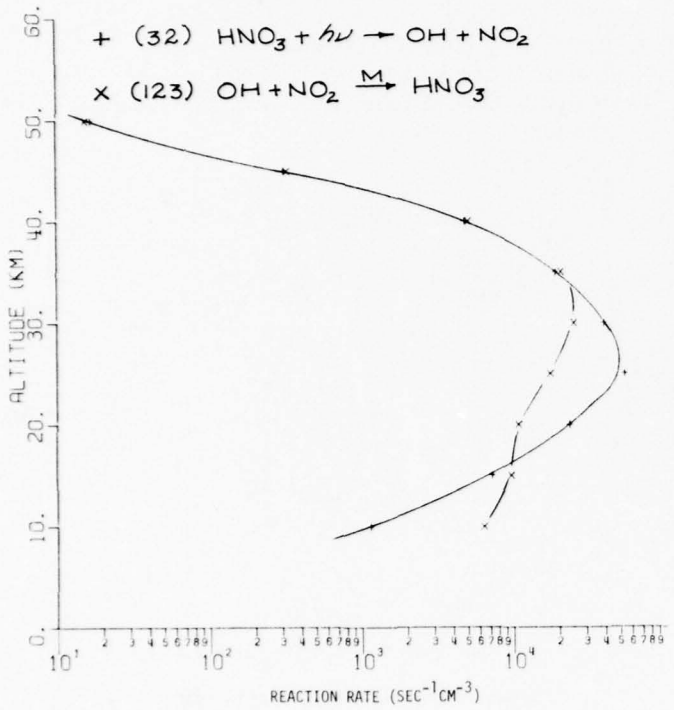

g

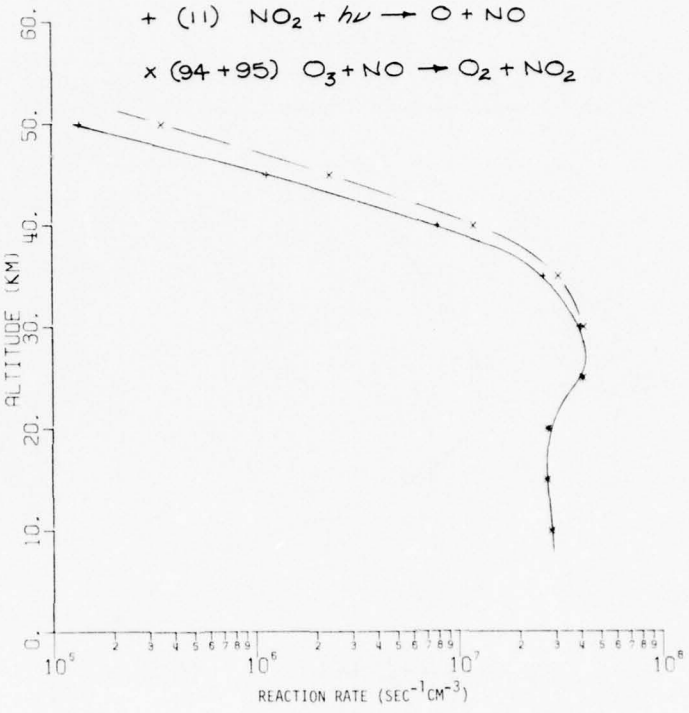

h

Figure 6. (cont)

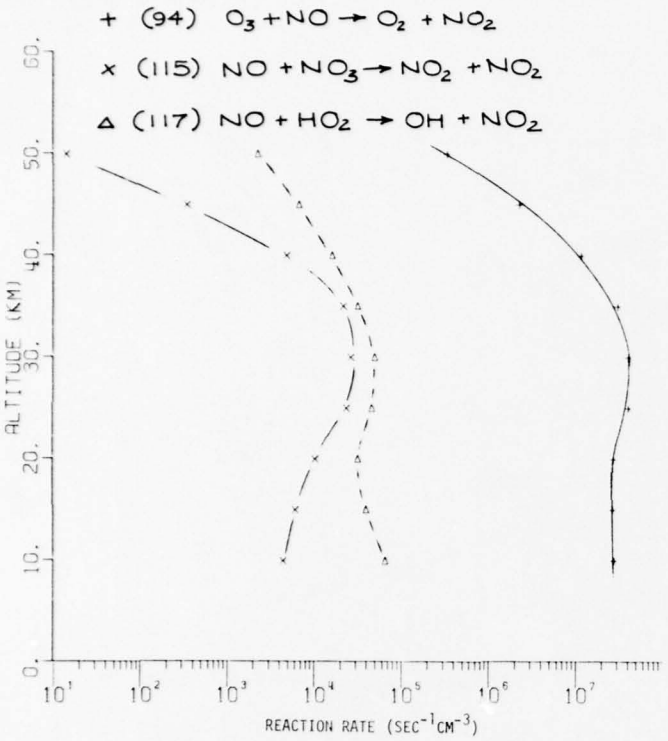

i

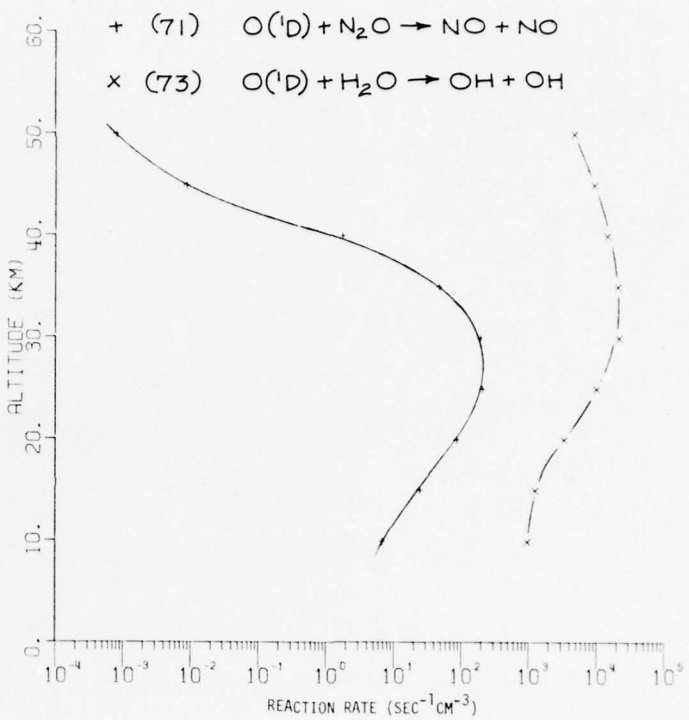

j

Figure 6. (cont)

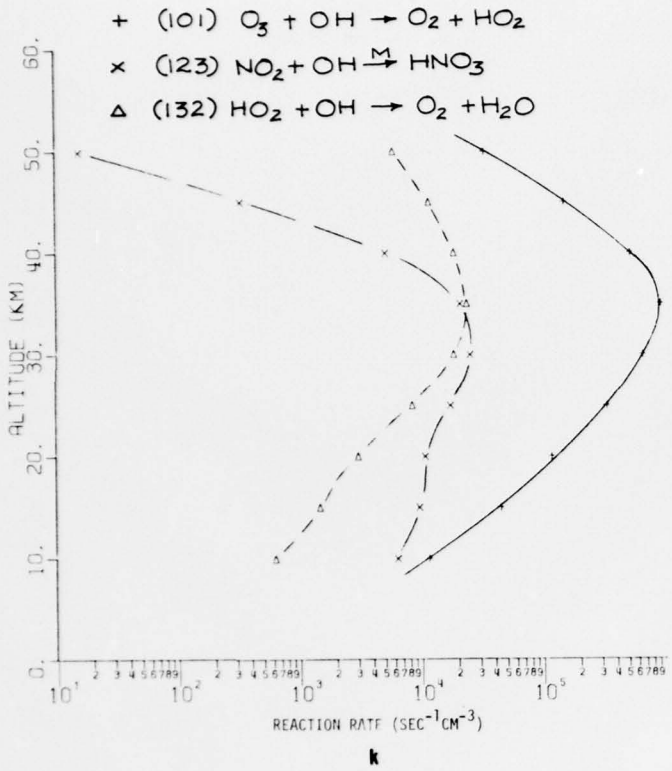

k

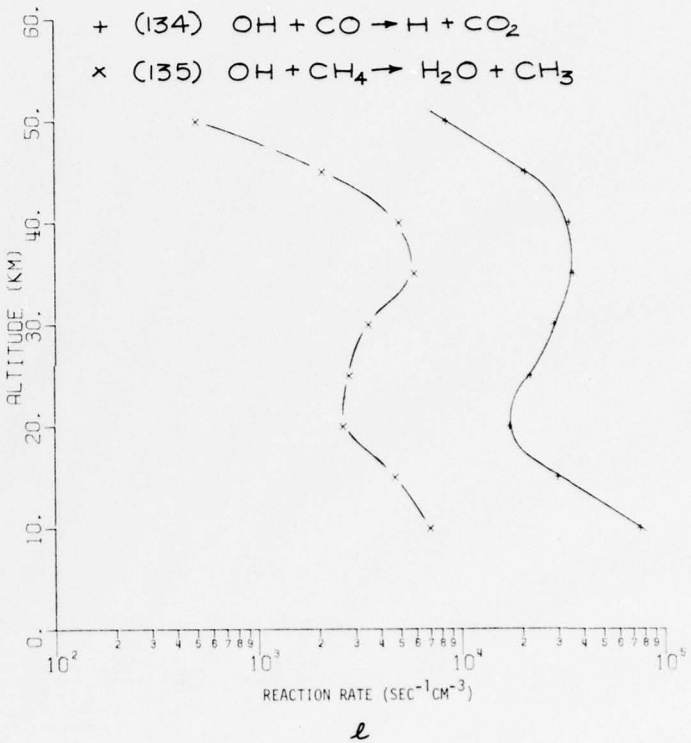

ℓ

Figure 6. (cont)

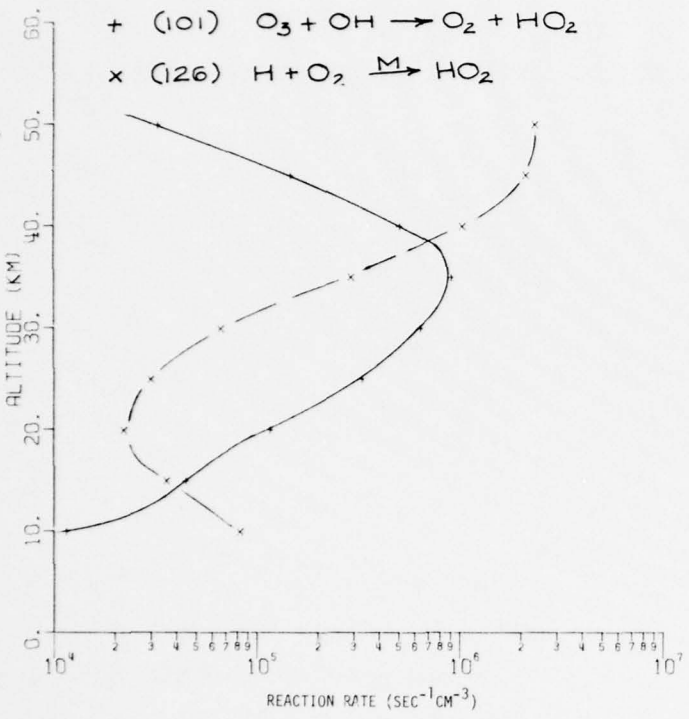

m

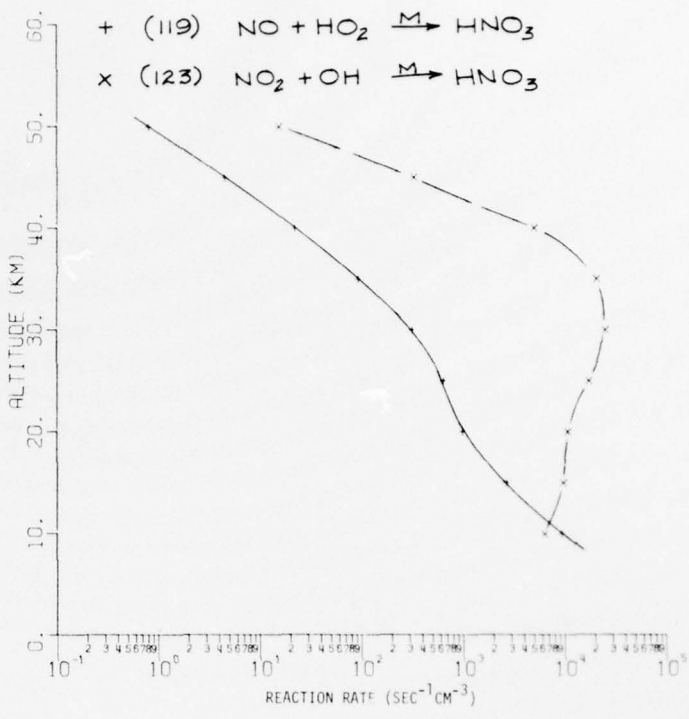

n

Figure 6. (cont)

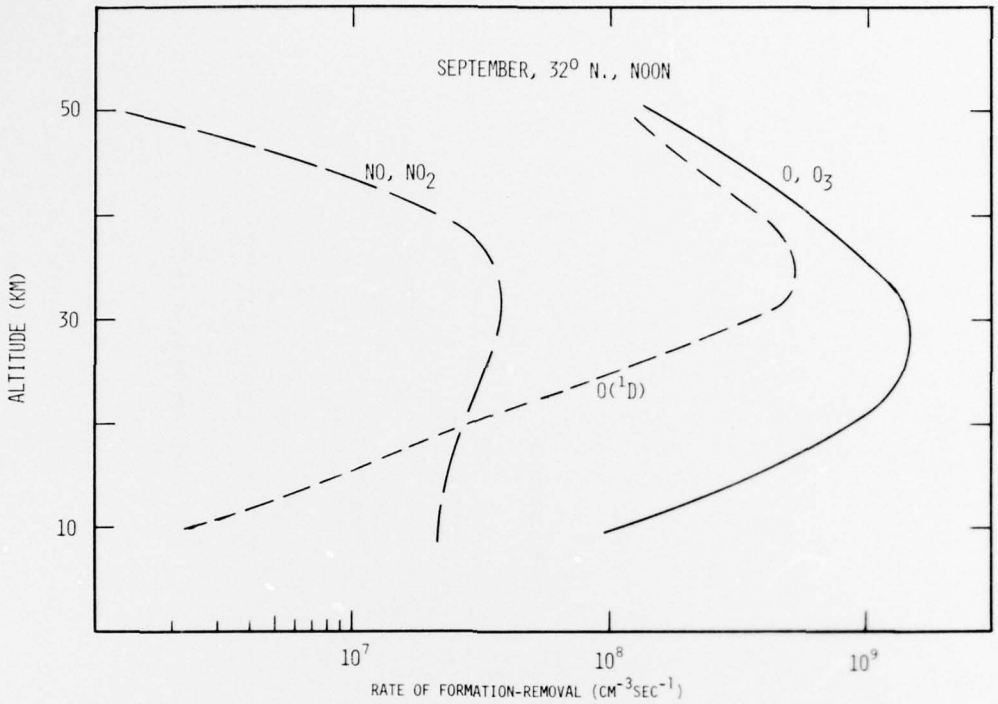

a

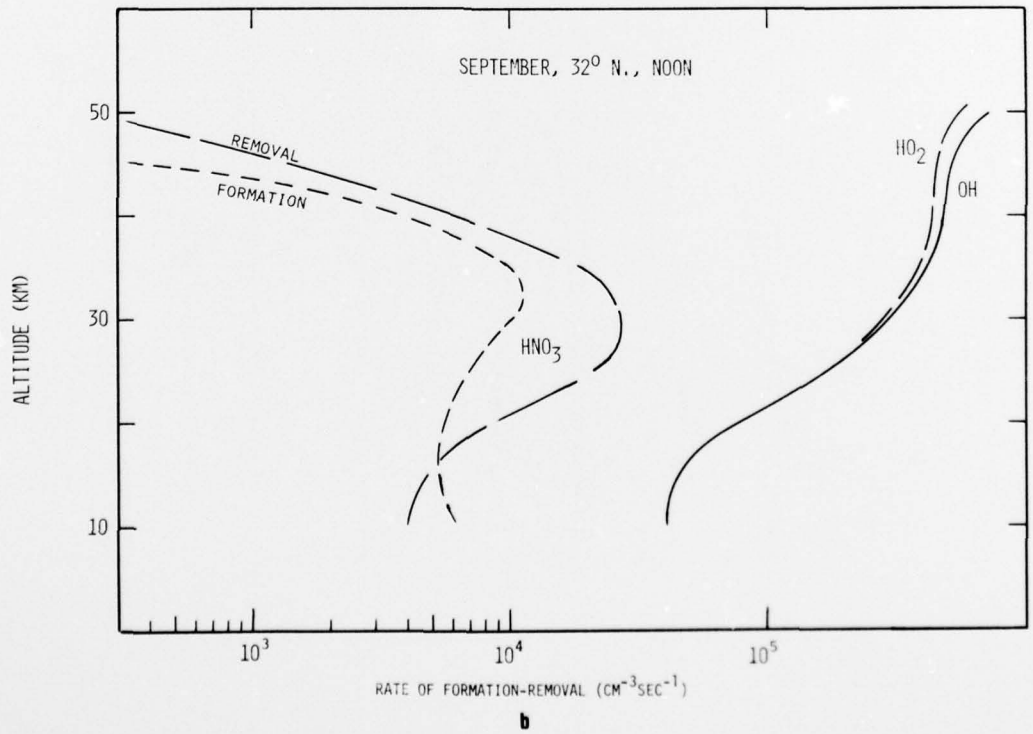

b

Figure 7. Total formation and removal rates.

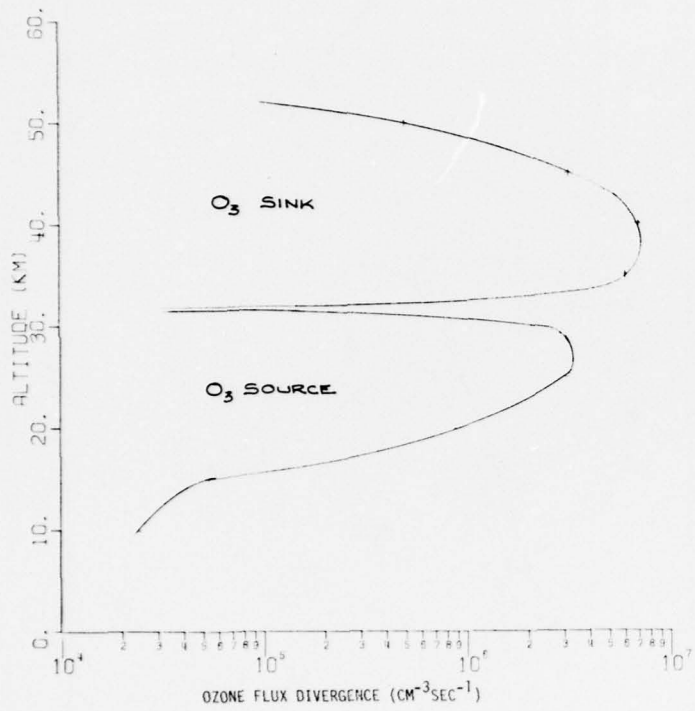

a

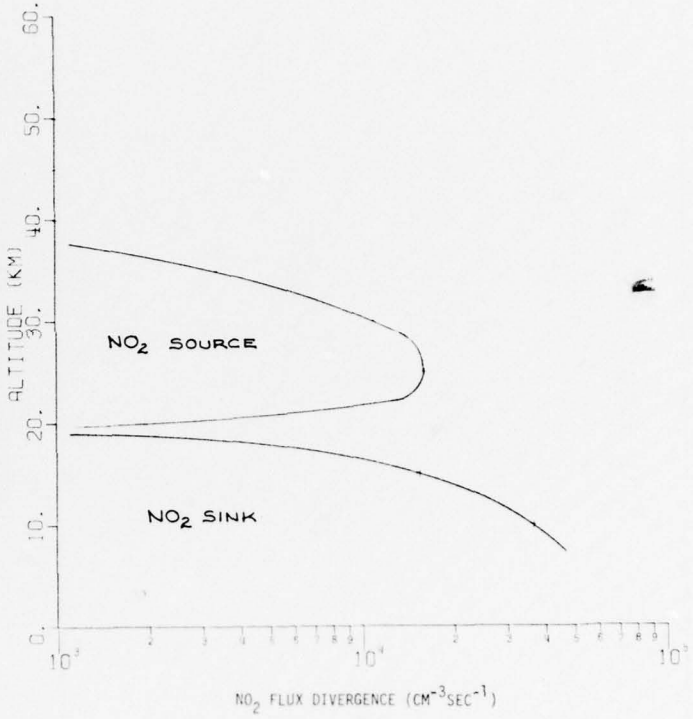

b

Figure 8. Transport contribution to particle densities.

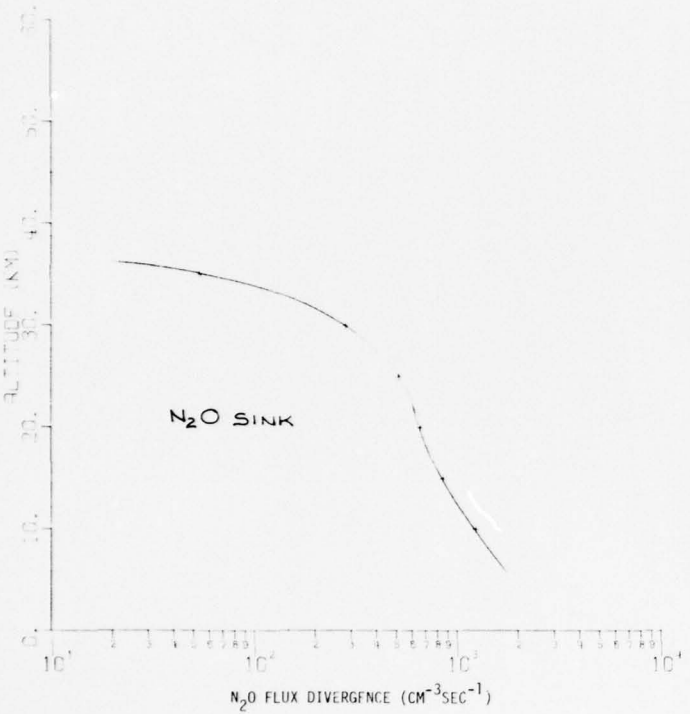

c

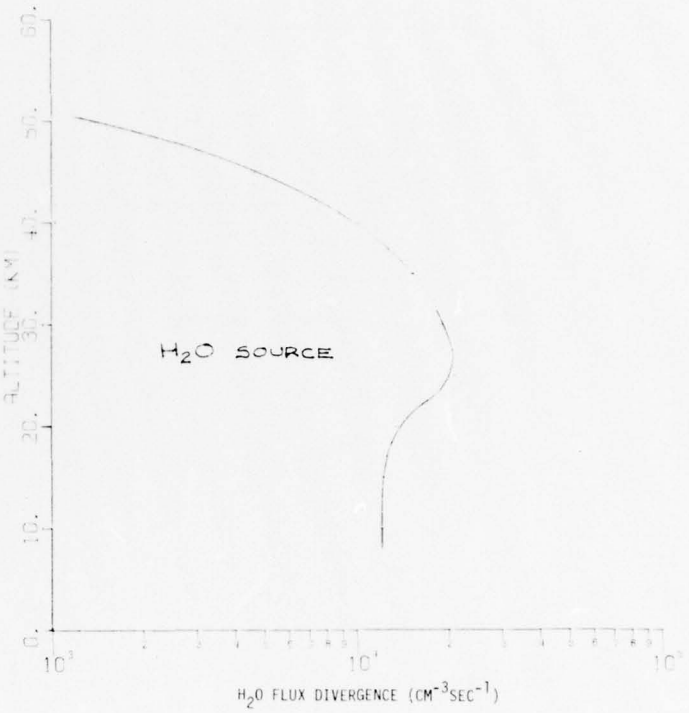

d

Figure 8. (cont)

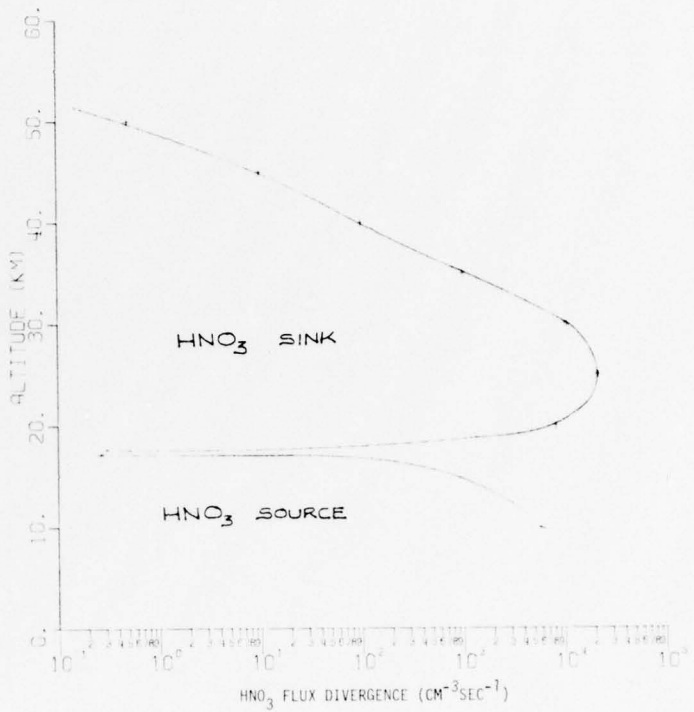

e

Figure 8. (cont)

REFERENCES

1. Ballard, Harold N., and Frank P. Hudson. "Stratospheric Composition Balloon-Borne Experiment, 18 September 1972." Research and Development Technical Report, ECOM-5554, Atmospheric Sciences Laboratory, US Army Electronics Command, White Sands Missile Range, NM, 1975.

2. Ballard, Harold N., Jose M. Serna, and Frank P. Hudson. "ANMAR: The ASL Numerical Model of Atmospheric Radiation, Composition and Dynamics." (in publication)

3. Ballard, Harold N. et al. "STRATCOM VI Experimental Results." ECOM Report, Atmospheric Sciences Laboratory, US Army Electronics Command, White Sands Missile Range, NM. (in preparation)

4. Collins, Jerry L. "STRATCOM-Related Photodissociation Rates and Solar Flux Intensities." Special Report SP5-76-UA-26, University of Texas at El Paso, El Paso, TX, 3 December 1976.

5. Gear, C. W. "The Automatic Integration of Ordinary Differential Equations." Communications of the ACM 14 (March 1971): 176.

6. Anderson, James G. "The Absolute Concentration of $O(^3P)$ in the Earth's Stratosphere." Geophysical Research Letters 2 (June 1975): 231.

7. Anderson, J. G. "The Absolute Concentration of $OH(X^2\pi)$ in the Earth's Atmosphere." Geophysical Research Letters 3 (March 1976): 165.

8. Lowenstein, Max. Private Communication, 1976.

9. Randhawa, J. S., and M. Izquierdo. Journal of Photochemistry 6, (1976): 147.

ATMOSPHERIC SCIENCES RESEARCH PAPERS

1. Lindberg, J.D., "An Improvement to a Method for Measuring the Absorption Coefficient of Atmospheric Dust and other Strongly Absorbing Powders," ECOM-5565, July 1975.
2. Avara, Elton, P., "Mesoscale Wind Shears Derived from Thermal Winds," ECOM-5566, July 1975.
3. Gomez, Richard B. and Joseph H. Pierluissi, "Incomplete Gamma Function Approximation for King's Strong-Line Transmittance Model," ECOM-5567, July 1975.
4. Blanco, A.J. and B.F. Engebos, "Ballistic Wind Weighting Functions for Tank Projectiles," ECOM-5568, August 1975.
5. Taylor, Fredrick J., Jack Smith, and Thomas H. Pries, "Crosswind Measurements through Pattern Recognition Techniques," ECOM-5569, July 1975.
6. Walters, D.L., "Crosswind Weighting Functions for Direct-Fire Projectiles," ECOM-5570, August 1975.
7. Duncan, Louis D., "An Improved Algorithm for the Iterated Minimal Information Solution for Remote Sounding of Temperature," ECOM-5571, August 1975.
8. Robbiani, Raymond L., "Tactical Field Demonstration of Mobile Weather Radar Set AN/TPS-41 at Fort Rucker, Alabama," ECOM-5572, August 1975.
9. Miers, B., G. Blackman, D. Langer, and N. Lorimier, "Analysis of SMS/GOES Film Data," ECOM-5573, September 1975.
10. Manquero, Carlos, Louis Duncan, and Rufus Bruce, "An Indication from Satellite Measurements of Atmospheric CO_2 Variability," ECOM-5574, September 1975.
11. Petracca, Carmine and James D. Lindberg, "Installation and Operation of an Atmospheric Particulate Collector," ECOM-5575, September 1975.
12. Avara, Elton P. and George Alexander, "Empirical Investigation of Three Iterative Methods for Inverting the Radiative Transfer Equation," ECOM-5576, October 1975.
13. Alexander, George D., "A Digital Data Acquisition Interface for the SMS Direct Readout Ground Station—Concept and Preliminary Design," ECOM-5577, October 1975.
14. Cantor, Israel, "Enhancement of Point Source Thermal Radiation Under Clouds in a Nonattenuating Medium," ECOM-5578, October 1975.
15. Norton, Colburn and Glenn Hoidale, "The Diurnal Variation of Mixing Height by Month over White Sands Missile Range, NM," ECOM-5579, November 1975.
16. Avara, Elton P., "On the Spectrum Analysis of Binary Data," ECOM-5580, November 1975.
17. Taylor, Fredrick J., Thomas H. Pries, and Chao-Huan Huang, "Optimal Wind Velocity Estimation," ECOM-5581, December 1975.
18. Avara, Elton P., "Some Effects of Autocorrelated and Cross-Correlated Noise on the Analysis of Variance," ECOM-5582, December 1975.
19. Gillespie, Patti S., R.L. Armstrong, and Kenneth O. White, "The Spectral Characteristics and Atmospheric CO_2 Absorption of the Ho^{+3}:YLF Laser at 2.05μm," ECOM-5583, December 1975.
20. Novlan, David J., "An Empirical Method of Forecasting Thunderstorms for the White Sands Missile Range," ECOM-5584, February 1976.
21. Avara, Elton P., "Randomization Effects in Hypothesis Testing with Autocorrelated Noise," ECOM-5585, February 1976.
22. Watkins, Wendell R., "Improvements in Long Path Absorption Cell Measurement," ECOM-5586, March 1976.
23. Thomas, Joe, George D. Alexander, and Marvin Dubbin, "SATTEL — An Army Dedicated Meteorological Telemetry System," ECOM-5587, March 1976.
24. Kennedy, Bruce W. and Delbert Bynum, "Army User Test Program for the RDT&E-XM-75 Meteorological Rocket," ECOM-5588, April 1976.

25. Barnett, Kenneth M., "A Description of the Artillery Meteorological Comparisons at White Sands Missile Range, October 1974 — December 1974 ('PASS' — Prototype Artillery [Meteorological] Subsystem)," ECOM-5589, April 1976.
26. Miller, Walter B., "Preliminary Analysis of Fall-of-Shot From Project 'PASS'," ECOM-5590, April 1976.
27. Avara, Elton P., "Error Analysis of Minimum Information and Smith's Direct Methods for Inverting the Radiative Transfer Equation," ECOM-5591, April 1976.
28. Yee, Young P., James D. Horn, and George Alexander, "Synoptic Thermal Wind Calculations from Radiosonde Observations Over the Southwestern United States," ECOM-5592, May 1976.
29. Duncan, Louis D. and Mary Ann Seagraves, "Applications of Empirical Corrections to NOAA-4 VTPR Observations," ECOM-5593, May 1976.
30. Miers, Bruce T. and Steve Weaver, "Applications of Meterological Satellite Data to Weather Sensitive Army Operations," ECOM-5594, May 1976.
31. Sharenow, Moses, "Redesign and Improvement of Balloon ML-566," ECOM-5595, June 1976.
32. Hansen, Frank V., "The Depth of the Surface Boundary Layer," ECOM-5596, June 1976.
33. Pinnick, R.G. and E.B. Stenmark, "Response Calculations for a Commercial Light-Scattering Aerosol Counter," ECOM-5597, July 1976.
34. Mason, J. and G.B. Hoidale, "Visibility as an Estimator of Infrared Transmittance," ECOM-5598, July 1976.
35. Bruce, Rufus E., Louis D. Duncan, and Joseph H. Pierluissi, "Experimental Study of the Relationship Between Radiosonde Temperatures and Radiometric-Area Temperatures," ECOM-5599, August 1976.
36. Duncan, Louis D., "Stratospheric Wind Shear Computed from Satellite Thermal Sounder Measurements," ECOM-5800, September 1976.
37. Taylor, F., P. Mohan, P. Joseph and T. Pries, "An All Digital Automated Wind Measurement System," ECOM-5801, September 1976.
38. Bruce, Charles, "Development of Spectrophones for CW and Pulsed Radiation Sources," ECOM-5802, September 1976.
39. Duncan, Louis D. and Mary Ann Seagraves, "Another Method for Estimating Clear Column Radiances," ECOM-5803, October 1976.
40. Blanco, Abel J. and Larry E. Traylor, "Artillery Meteorological Analysis of Project Pass," ECOM-5804, October 1976.
41. Miller, Walter and Bernard Engebos, "A Mathematical Structure for Refinement of Sound Ranging Estimates," ECOM-5805, November, 1976.
42. Gillespie, James B. and James D. Lindberg, "A Method to Obtain Diffuse Reflectance Measurements from 1.0 to 3.0μm Using a Cary 17I Spectrophotometer," ECOM-5806, November 1976.
43. Rubio, Roberto and Robert O. Olsen, "A Study of the Effects of Temperature Variations on Radio Wave Absorption," ECOM-5807, November 1976.
44. Ballard, Harold N., "Temperature Measurements in the Stratosphere from Balloon-Borne Instrument Platforms, 1968-1975," ECOM-5808, December, 1976.
45. Monahan, H.H., "An Approach to the Short-Range Prediction of Early Morning Radiation Fog," ECOM-5809, January 1977.
46. Engebos, Bernard Francis, "Introduction to Multiple State Multiple Action Decision Theory and Its Relation to Mixing Structures," ECOM-5810, January 1977.
47. Low, Richard D.H., Effects of Cloud Particles on Remote Sensing from Space in the 10-Micrometer Infrared Region, ECOM-5811, January 1977.
48. Bonner, Robert S. and R. Newton, "Application of the AN/GVS-5 Laser Rangefinder to Cloud Base Height Measurements," ECOM-5812, February 1977.

49. Rubio, Roberto, "Lidar Detection of Subvisible Reentry Vehicle Erosive Atmospheric Material," ECOM-5813, March 1977.

50. Low, Richard D.H. and J.D. Horn, "Mesoscale Determination of Cloud-Top Height: Problems and Solutions," ECOM-5814, March 1977.

51. Duncan, Louis D. and Mary Ann Seagraves, "Evaluation of the NOAA-4 VTPR Thermal Winds for Nuclear Fallout Predictions," ECOM-5815, March 1977.

52. Randhawa, Jagir S., M. Izquierdo, Carlos McDonald and Zvi Salpeter, "Stratospheric Ozone Density as Measured by a Chemiluminescent Sensor During the Stratcom VI-A Flight," ECOM-5816, April 1977.

53. Rubio, Roberto and Mike Izquierdo, "Measurements of Net Atomospheric Irradiance in the 0.7- to 2.8-Micrometer Infrared Region," ECOM-5817, May 1977.

54. Ballard, Harold N., José M. Serna, and Frank P. Hudson Consultant for Chemical Kinetics, "Calculation of Selected Atmospheric Composition Parameters for the Mid-Latitude, September Stratosphere," ECOM-5818, May 1977.

DISTRIBUTION LIST

Director
US Army Ballistic Research Laboratory
ATTN: DRDAR-BLB, Dr. G. E. Keller
Aberdeen Proving Ground, MD 21005

Air Force Weapons Laboratory
ATTN: Technical Library (SUL)
Kirtland AFB, NM 87117

Commander
Headquarters, Fort Huachuca
ATTN: Tech Ref Div
Fort Huachuca, AZ 85613

6585 TG/WE
Holloman AFB, NM 88330

Commandant
US Army Field Artillery School
ATTN: Morris Swett Tech Library
Fort Sill, OK 73503

Commandant
USAFAS
ATTN: ATSF-CD-MT (Mr. Farmer)
Fort Sill, OK 73503

Director
US Army Engr Waterways Exper Sta
ATTN: Library Branch
Vicksburg, MS 39180

Commander
US Army Electronics Command
ATTN: DRSEL-CT-S (Dr. Swingle)
Fort Monmouth, NJ 07703
03

CPT Hugh Albers, Exec Sec
Interdept Committee on Atmos Sci
Fed Council for Sci & Tech
National Sci Foundation
Washington, DC 20550

Inge Dirmhirn, Professor
Utah State University, UMC 48
Logan, UT 84322

HQDA (DAEN-RDM/Dr. De Percin)
Forrestal Bldg
Washington, DC 20314

Commander
US Army Aviation Center
ATTN: ATZQ-D-MA
Fort Rucker, AL 36362

CO, USA Foreign Sci & Tech Center
ATTN: DRXST-ISI
220 7th Street, NE
Charlottesville, VA 22901

Director
USAE Waterways Experiment Station
ATTN: Library
PO Box 631
Vicksburg, MS 39180

US Army Research Office
ATTN: DRXRO-IP
PO Box 12211
Research Triangle Park, NC 27709

Mr. William A. Main
USDA Forest Service
1407 S. Harrison Road
East Lansing, MI 48823

Library-R-51-Tech Reports
Environmental Research Labs
NOAA
Boulder, CO 80302

Commander
US Army Dugway Proving Ground
ATTN: MT-S
Dugway, UT 84022

HQ, ESD/DRI/S-22
Hanscom AFB
MA 01731

Head, Atmospheric Rsch Section
National Science Foundation
1800 G. Street, NW
Washington, DC 20550

Office, Asst Sec Army (R&D)
ATTN: Dep for Science & Tech
HQ, Department of the Army
Washington, DC 20310

Commander
US Army Satellite Comm Agc
ATTN: DRCPM-SC-3
Fort Monmouth, NJ 07703

Sylvania Elec Sys Western Div
ATTN: Technical Reports Library
PO Box 205
Mountain View, CA 94040

William Peterson
Research Association
Utah State University, UNC 48
Logan, UT 84322

Defense Communications Agency
Technical Library Center
Code 205
Washington, DC 20305

Dr. A. D. Belmont
Research Division
PO Box 1249
Control Data Corp
Minneapolis, MN 55440

Commander
US Army Electronics Command
ATTN: DRSEL-WL-D1
Fort Monmouth, NJ 07703

Commander
ATTN: DRSEL-VL-D
Fort Monmouth, NJ 07703

Meteorologist in Charge
Kwajalein Missile Range
PO Box 67
APO
San Francisco, CA 96555

The Library of Congress
ATTN: Exchange & Gift Div
Washington, DC 20540
2

US Army Liaison Office
MIT-Lincoln Lab, Library A-082
PO Box 73
Lexington, MA 02173

Dir National Security Agency
ATTN: TDL (C513)
Fort George G. Meade, MD 20755

Director, Systems R&D Service
Federal Aviation Administration
ATTN: ARD-54
2100 Second Street, SW
Washington, DC 20590

Commander
US Army Missile Command
ATTN: DRSMI-RRA, Bldg 7770
Redstone Arsenal, AL 35809

Dir of Dev & Engr
Defense Systems Div
ATTN: SAREA-DE-DDR
H. Tannenbaum
Edgewood Arsenal, APG, MD 21010

Naval Surface Weapons Center
Technical Library & Information
Services Division
White Oak, Silver Spring, MD
20910

Dr. Frank D. Eaton
PO Box 3038
Universtiy Station
Laramie, Wyoming 82071

Rome Air Development Center
ATTN: Documents Library
TILD (Bette Smith)
Griffiss Air Force Base, NY 13441

National Weather Service
National Meteorological Center
World Weather Bldg - 5200 Auth Rd
ATTN: Mr. Quiroz
Washington, DC 20233

USAFETAC/CB (Stop 825)
Scott AFB
IL 62225

Director
Defense Nuclear Agency
ATTN: Tech Library
Washington, DC

Director
Development Center MCDEC
ATTN: Firepower Division
Quantico, VA 22134

Environmental Protection Agency
Meteorology Laboratory
Research Triangle Park, NC
27711

Commander
US Army Electronics Command
ATTN: DRSEL-GG-TD
Fort Monmouth, NJ 07703

Commander
US Army Ballistic Rsch Labs
ATTN: DRXBR-IB
APG, MD 21005

Dir, US Naval Research Lab
Code 5530
Washington, DC 20375

Mil Assistant for
Environmental Sciences
DAD (E & LS), 3D129
The Pentagon
Washington, DC 20301

The Environmental Rsch
Institute of MI
ATTN: IRIA Library
PO Box 618
Ann Arbor, MI 48107

Armament Dev & Test Center
ADTC (DLOSL)
Eglin AFB, Florida 32542

Range Commanders Council
ATTN: Mr. Hixon
PMTC Code 3252
Pacific Missile Test Center
Point Mugu, CA 93042

Commander
Eustis Directorate
US Army Air Mobility R&D Lab
ATTN: Technical Library
Fort Eustis, VA 23604

Commander
Frankford Arsenal
ATTN: SARFA-FCD-O, Bldg 201-2
Bridge & Tarcony Sts
Philadelphia, PA 19137

Director, Naval Oceanography and
Meteorology
National Space Technology Laboratories
Bay St Louis, MS 39529

Commander
US Army Electronics Command
ATTN: DRSEL-CT-S
Fort Monmouth, NJ 07703

Commander
USA Cold Regions Test Center
ATTN: STECR-OP-PM
APO Seattle 98733

Redstone Scientific Information Center
ATTN: DRDMI-TBD
US Army Missile Res & Dev Command
Redstone Arsenal, AL 35809

Commander
AFWL/WE
Kirtland AFB, NM 87117

Naval Surface Weapons Center
Code DT-22 (Ms. Greeley)
Dahlgren, VA 22448

Commander
Naval Ocean Systems Center
ATTN: Research Library
San Diego, CA 92152

Commander
US Army INSCOM
ATTN: IARDA-OS
Arlington Hall Station
Arlington, VA 22212

Commandant
US Army Field Artillery School
ATTN: ATSF-CF-R
Fort Sill, OK 73503

Commander
US Army Tropic Test Center
ATTN: STETC-MO (Tech Library)
APO New York 09827

Commanding Officer
Naval Research Laboratory
Code 2627
Washington, DC 20375

Defense Documentation Center
ATTN: DDC-TCA
Cameron Station (Bldg 5)
Alexandria, Virginia 22314
12

Commander
US Army Test and Evaluation Command
ATTN: Technical Library
White Sands Missile Range, NM 88002

US Army Nuclear Agency
ATTN: MONA-WE
Fort Belvoir, VA 22060

Commander
US Army Proving Ground
ATTN: Technical Library
Bldg 2100
Yuma, AZ 85364

Office, Asst Sec Army (R&D)
ATTN: Dep for Science & Tech
HQ, Department of the Army
Washington, DC 20310

☆ U.S. GOVERNMENT PRINTING OFFICE: 1977—777-022/24